Summer school on Epitaxy
MATEPI 2025
Porquerolles June 22-27 2025

Chapter II Epitaxy : experimental description

II.6 Comparison of oxide and semiconductor epitaxy and oxide/semiconductor integration

Guillaume Saint-Girons

INL-UMR5270/CNRS, Ecole Centrale de Lyon, 36 avenue Guy de Collongue 69134 Ecully cedex, France

Outlook

Introduction

a. Accommodation/growth mode and material-substrate dissimilarity
b. Oxides and semiconductors : comparison of some properties relevant to epitaxy

Increasing dissimilarity

Strained 2D growth and plastic relaxation

a. Dislocation mediated plastic relaxation process
b. Plastic relaxation : oxides vs semiconductors
c. Some exotic effects of oxide epitaxy related to epitaxial strain

Strain free 3D growth

a. Strain-induced 3D growth: Stranski-Krastanov growth mode
b. Interface induced 3D growth

Highly dissimilar epitaxial systems

a. Indirect epitaxial relationships
b. Mismatch accommodation via interfacial dislocation networks
c. Interface chemical reactions

Conclusion and future challenges

a. Oxide/Si templates: a mature technology for integration
b. MBE for oxide growth

Introduction

Accommodation/growth mode and material-substrate dissimilarity

Condensation of a vapor of A on a substrate B : energy balance

$\boldsymbol{\Delta\mu}$: Chemical potential difference

$\boldsymbol{\gamma_A}$: Material surface energy

$\boldsymbol{\gamma_B}$: Substrate surface energy

$\boldsymbol{\gamma_{AB}}$: Interface energy

$\boldsymbol{E_{dis}}$: Interface dislocation energy

$\boldsymbol{E_{el}}$: Elastic energy

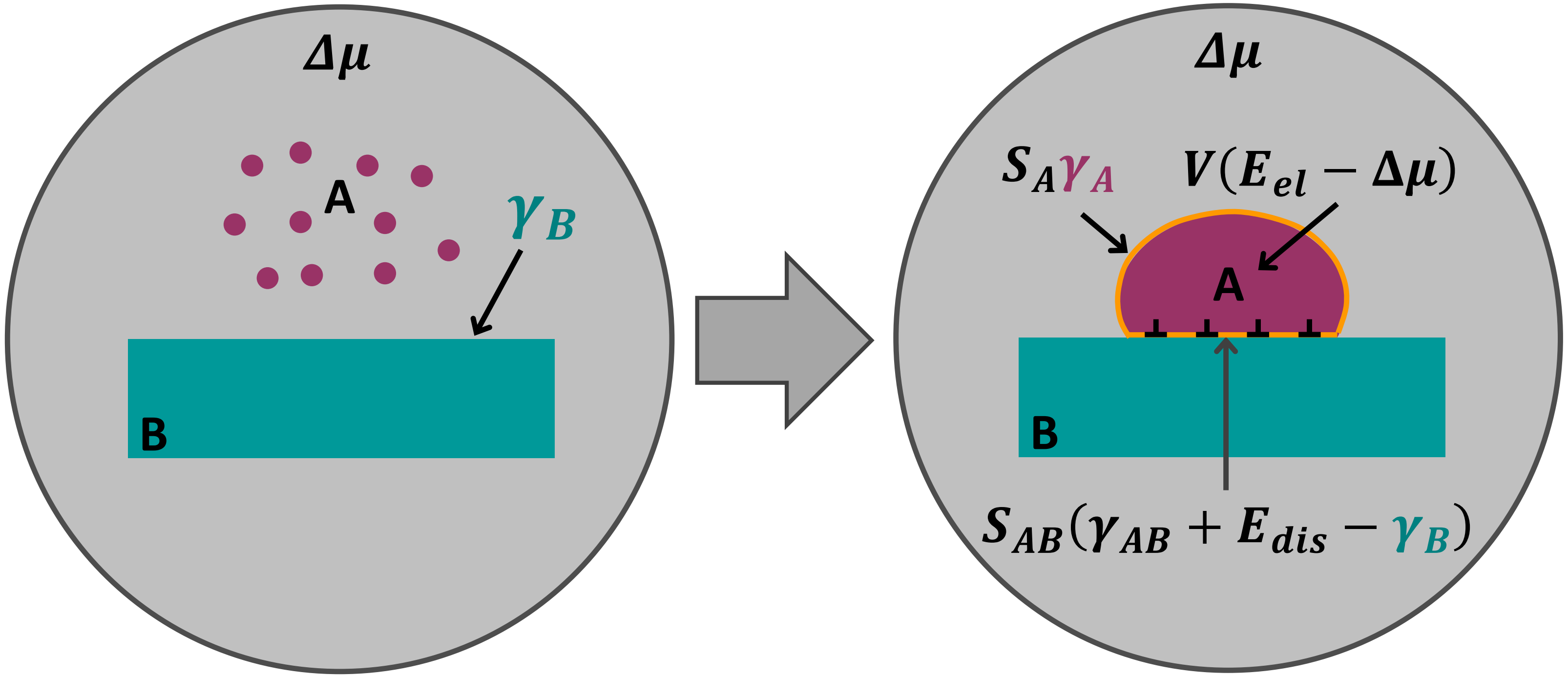

$\boldsymbol{V}$: Droplet volume

$\boldsymbol{S_A}$: Droplet surface

$\boldsymbol{S_{AB}}$: Interface area

Nucleation free enthalpy : $\boldsymbol{\Delta G = V(E_{el} - \Delta\mu) + S_{AB}(\gamma_{AB} + E_{dis} - \gamma_B) + S_A\gamma_A}$

G. Wulf, Z. Kristallog. ***34****, 449 (1901), P. Müller and R. Kern, Surf. Sci.* ***457****, 229 (2000)*

Introduction

Accommodation/growth mode and material-substrate dissimilarity

Surface and interface energies

I. Markov, Mat. Chem. Phys. ***36****, 1 (1993)*

N_B B-B bonds/m^2
Energy E_{BB}

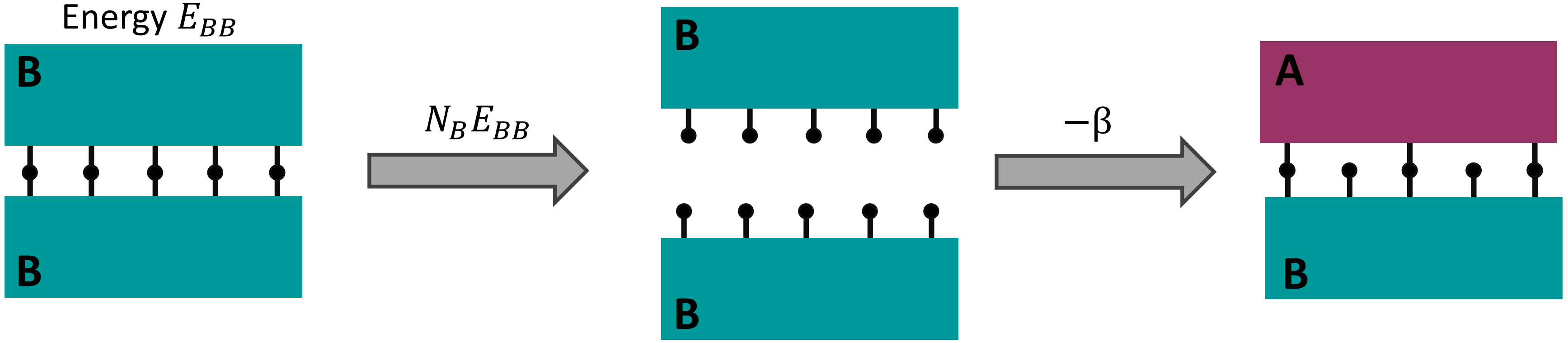

Energy cost E_{tot}

$$N_B E_{BB} + N_A E_{AA} - 2xN_B E_{AB}$$

Interface energy γ_{AB}

$$\gamma_{AB} = \frac{E_{tot}}{2} = \gamma_A + \gamma_B - \beta$$

$$= N_B \left[\frac{xE_{AA}}{2} + \frac{E_{BB}}{2} - min(x,1)E_{AB} \right]$$

Notwithstanding surface relaxation mechanisms

Surface energy γ_B (γ_A)

$$\gamma_B \sim \frac{N_B E_{BB}}{2}$$

Adhesion energy β

$xN_B E_{AB}$ $if\ x < 1$

$N_B E_{AB}$ $if\ x > 1$

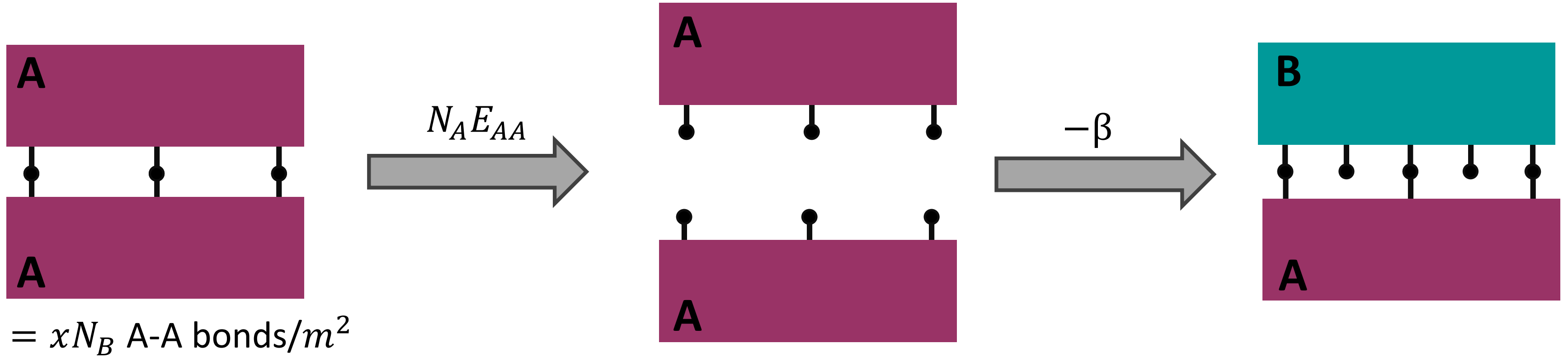

$N_A = xN_B$ A-A bonds/m^2
Energy E_{AA}

Homoepitaxy: $\gamma_{AB} = 0$

Strong adhesion: $\gamma_{AB} < 0$

$$\frac{xE_{AA} + E_{BB}}{2} < min(x,1)E_{AB}$$

Low adhesion: $\gamma_{AB} > 0$

$$\frac{xE_{AA} + E_{BB}}{2} > min(x,1)E_{AB}$$

Introduction

Accommodation/growth mode and material-substrate dissimilarity

Elastic energy

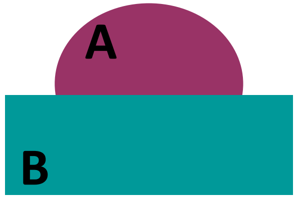

$$E_{el} = \frac{Y_A}{1-\nu_A} m^2 \left(1 - e^{-2k/p}\right)$$

Y_A: Young modulus
ν_A: Poisson ratio
$m = \frac{a_A - a_B}{a_B}$: lattice mismatch
p: droplet aspect ratio
k: 0.073 for a flat cylinder, 0.082 for a spherical cap

*K. Tillmann and A. Förster, Thin Solid Films **368**, 93, (2000)*

Interfacial dislocation network energies

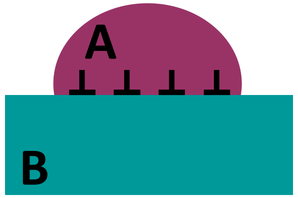

$$E_{dis} = mb \frac{Y_A Y_B}{Y_A(1+\nu_A) + Y_B(1+\nu_B)} \left(\frac{1}{4\pi} ln \frac{R_c}{b} + 0.1\right)$$

b: Burger vector norm
R_c: Cut-off radius (1/2 distance between 2 successive dislocations or droplet height)

J.W Matthews, « dislocations in solids », Academic Press, New York (1989)

Introduction

Accommodation/growth mode and material-substrate dissimilarity

Critical volume V_c

No stable nucleus with $V < V_c$

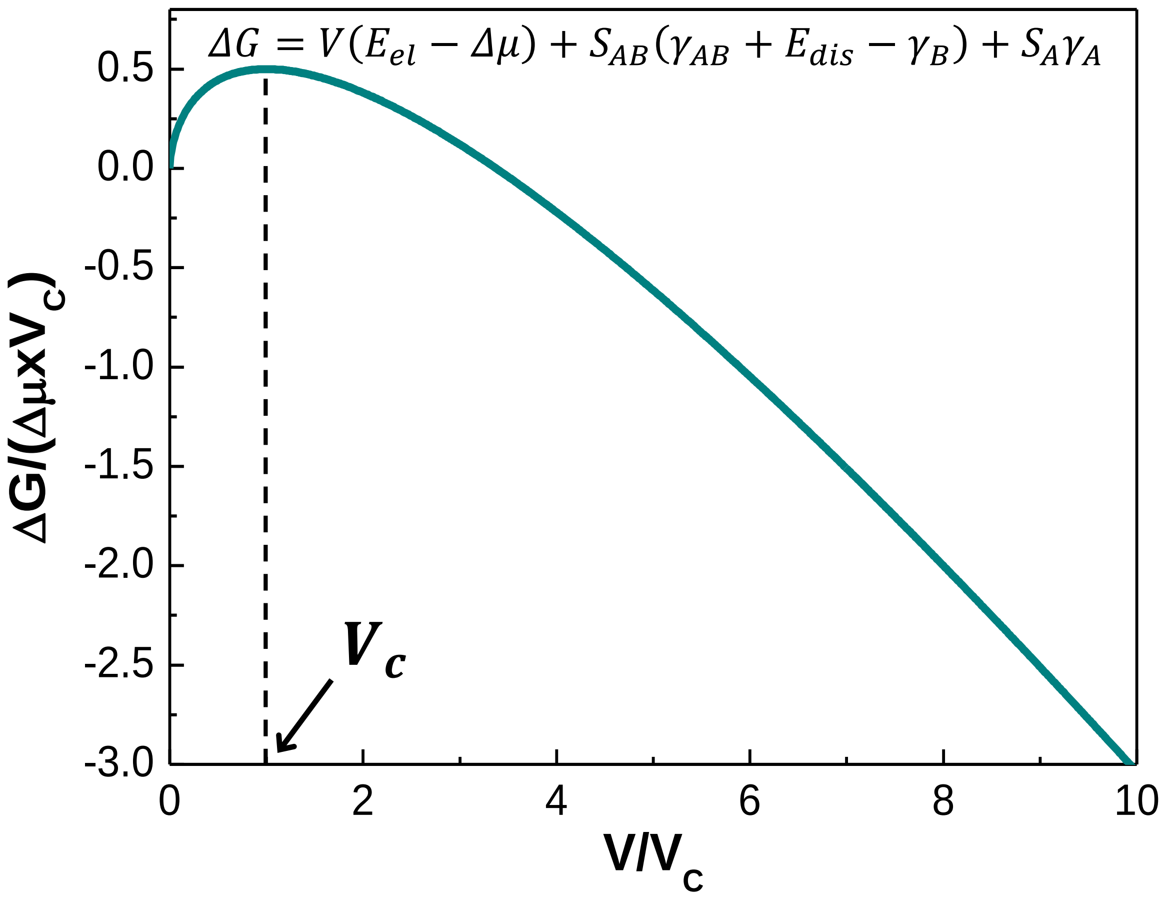

The observed configuration is that minimizing V_c

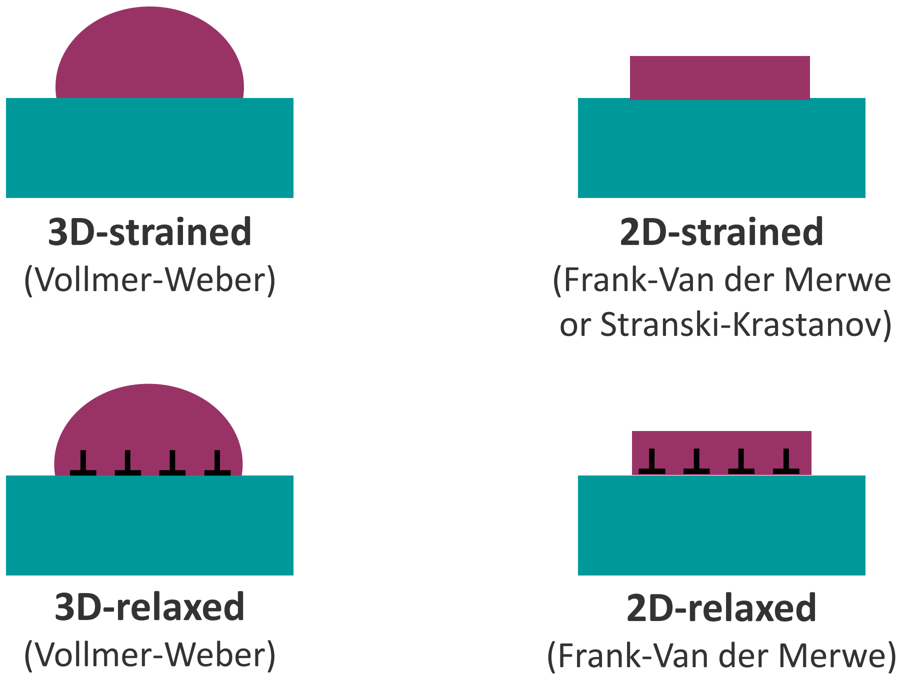

Introduction

Accommodation/growth mode and material-substrate dissimilarity

Wetting: $\alpha_B = \frac{\gamma_{AB} - \gamma_B}{\gamma_A}$

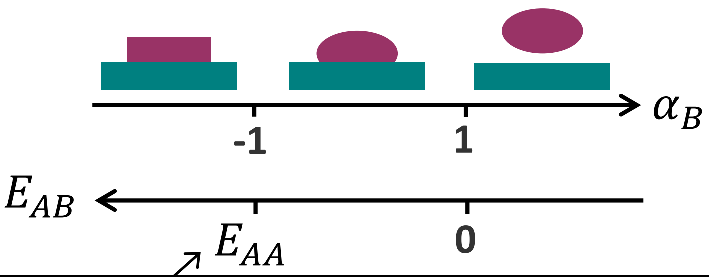

xE_{AA}
if $x > 1$

Critical volume V_c

Geometrical factors

$$V_c = \left(\frac{2}{3} L \frac{\alpha_B f + g}{1 - \alpha_C}\right)^3$$

Nucleus radius (@ 0 strain):

$L = \frac{\gamma_A}{\Delta_\mu}$

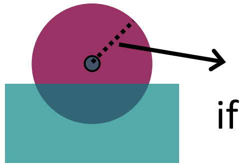

$2L$
if $\alpha_C = 0$

Strain: $\alpha_C = \frac{E_{el}}{\Delta_\mu}$

$\alpha_C > 1$: no condensation

Introduction

Accommodation/growth mode and material-substrate dissimilarity

Phase diagram for epitaxy ($\gamma_A = 1\ J/m^2$)

*Saint-Girons et al., Phys. Rev. B **80**, 155308 (2009)*

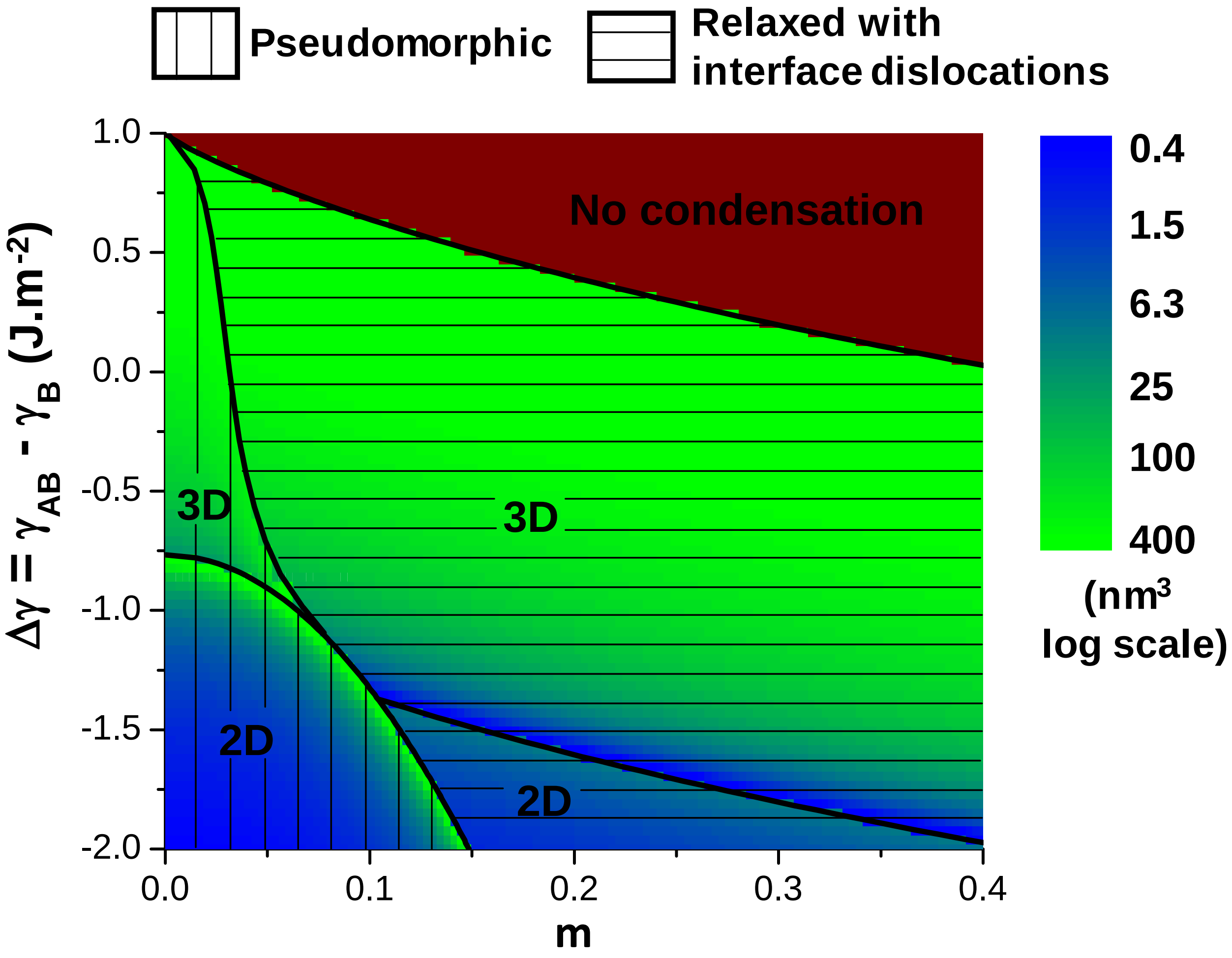

Where on this diagram are the Ox/Ox, SC/SC and Ox/SC epitaxial systems?

Introduction

Oxide and semiconductors : some properties relevant to epitaxy

$\boldsymbol{m}$**?**

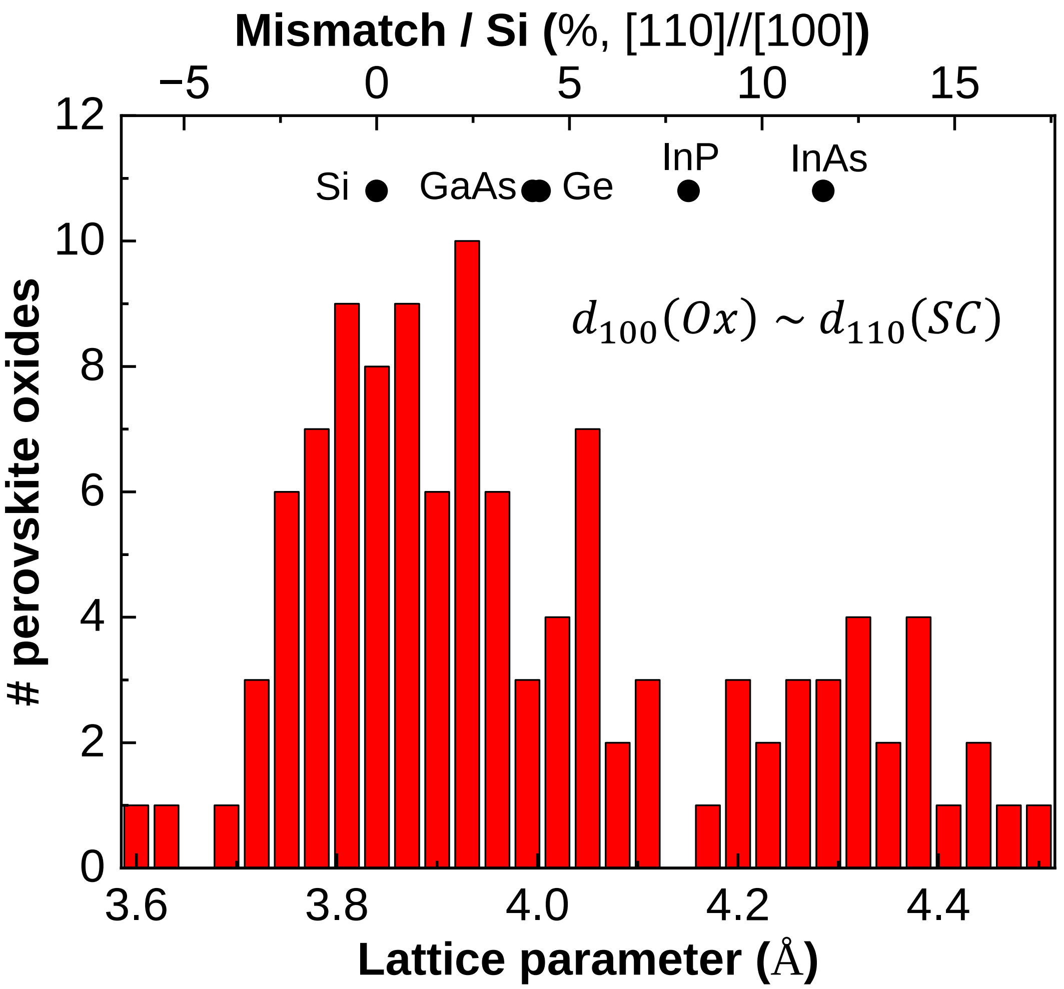

$\boldsymbol{\gamma_{AB} - \gamma_B}$**?**

$$\gamma_{AB} - \gamma_B = \gamma_A - \beta \sim N_B \left(\frac{xE_{AA}}{2} - min(x,1)E_{AB} \right)$$

$$\gamma_{AB} - \gamma_B \begin{cases} = -\gamma_A \text{ (homoepitaxy)} \\ < -\gamma_A \text{ if } xE_{AB} > \frac{xE_{AA}}{min(x,1)} \\ > -\gamma_A \text{ otherwise} \end{cases}$$

γ_A typically ranges from 0.8 to 1.6 J/m^2

Introduction

Oxide and semiconductors : some properties relevant to epitaxy

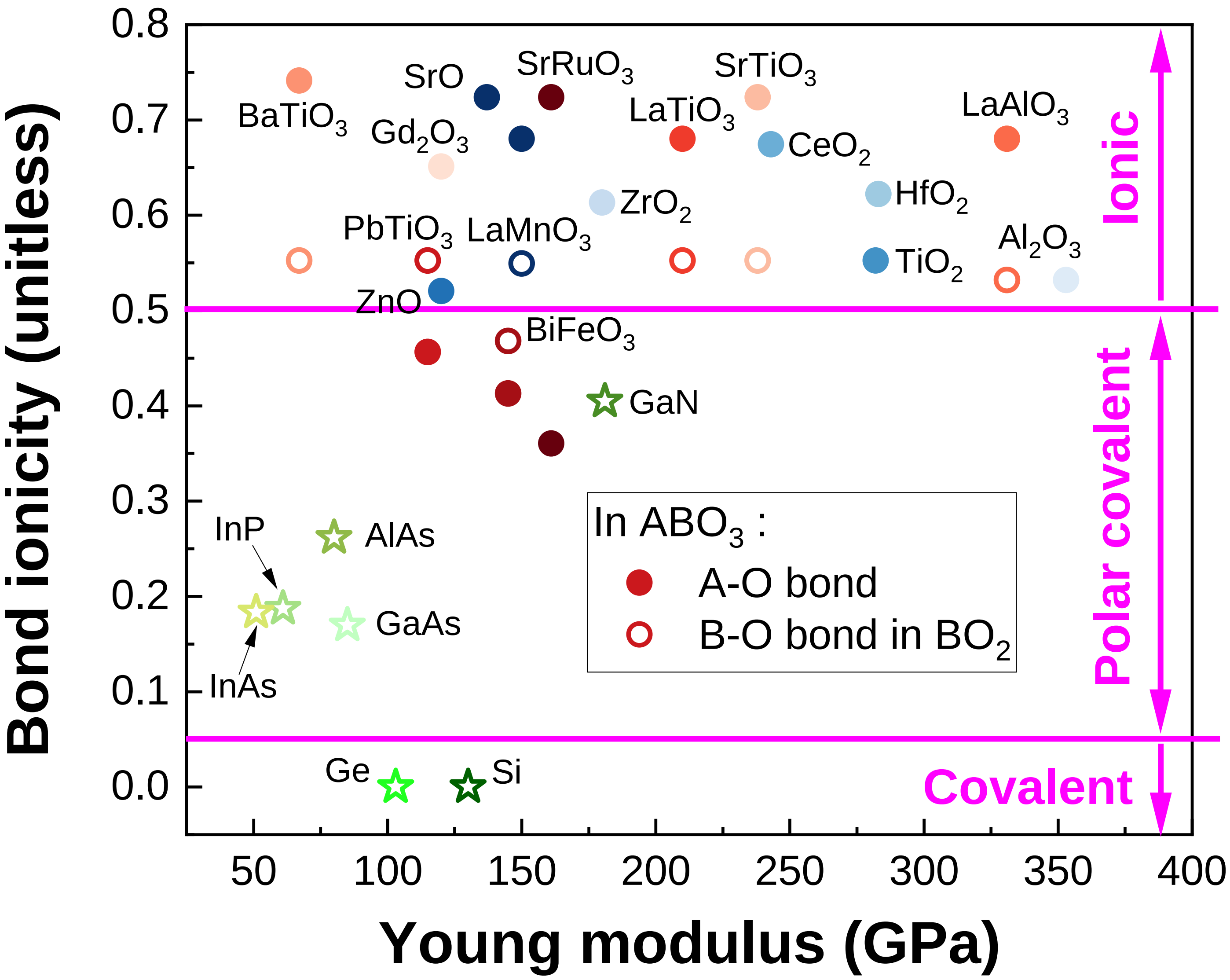

Young modulus:
$Y(Oxides) > Y(Semiconductors)$

Bond ionicity:
$\Delta EN(Oxides) > \Delta EN(Semiconductors)$

Dislocation formation and progagation hindered in oxides

Introduction

Exploring the phase diagram with semiconductor and oxide examples

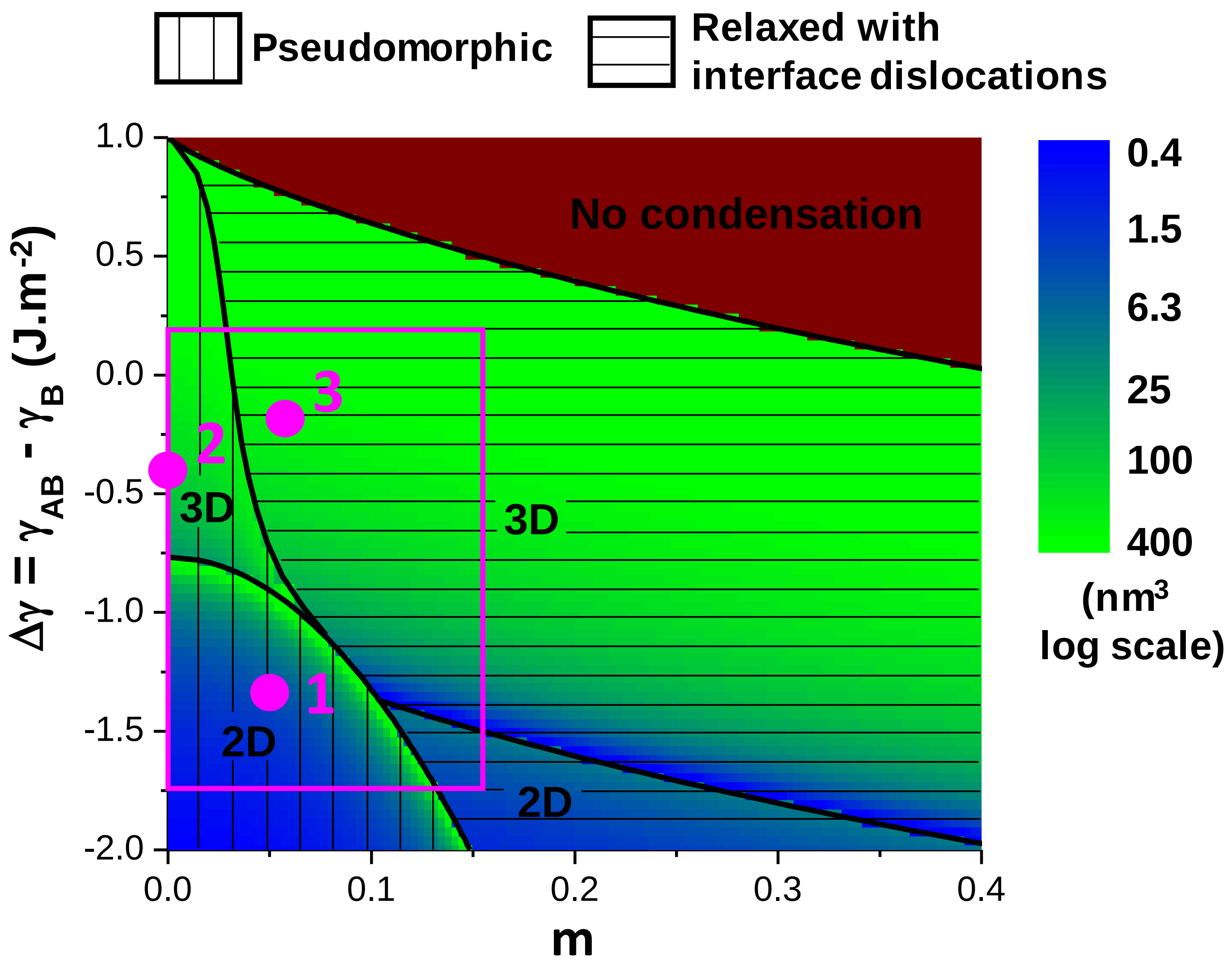

1. Strained 2D growth and plastic relaxation

2. Strain free 3D growth mode

3. Highly dissimilar epitaxial systems

1. Strained 2D growth and plastic relaxation

a. Dislocation mediated plastic relaxation

b. Plastic relaxation: comparison of oxides and semiconductors

c. Other effects of epitaxial strain on oxide growth

- $BaTiO_3$ ferroelectric domain structure
- Strain-assisted phase selection during Carpy-Gally compound growth

Strained 2D growth and plastic relaxation

Dislocation mediated plastic relaxation

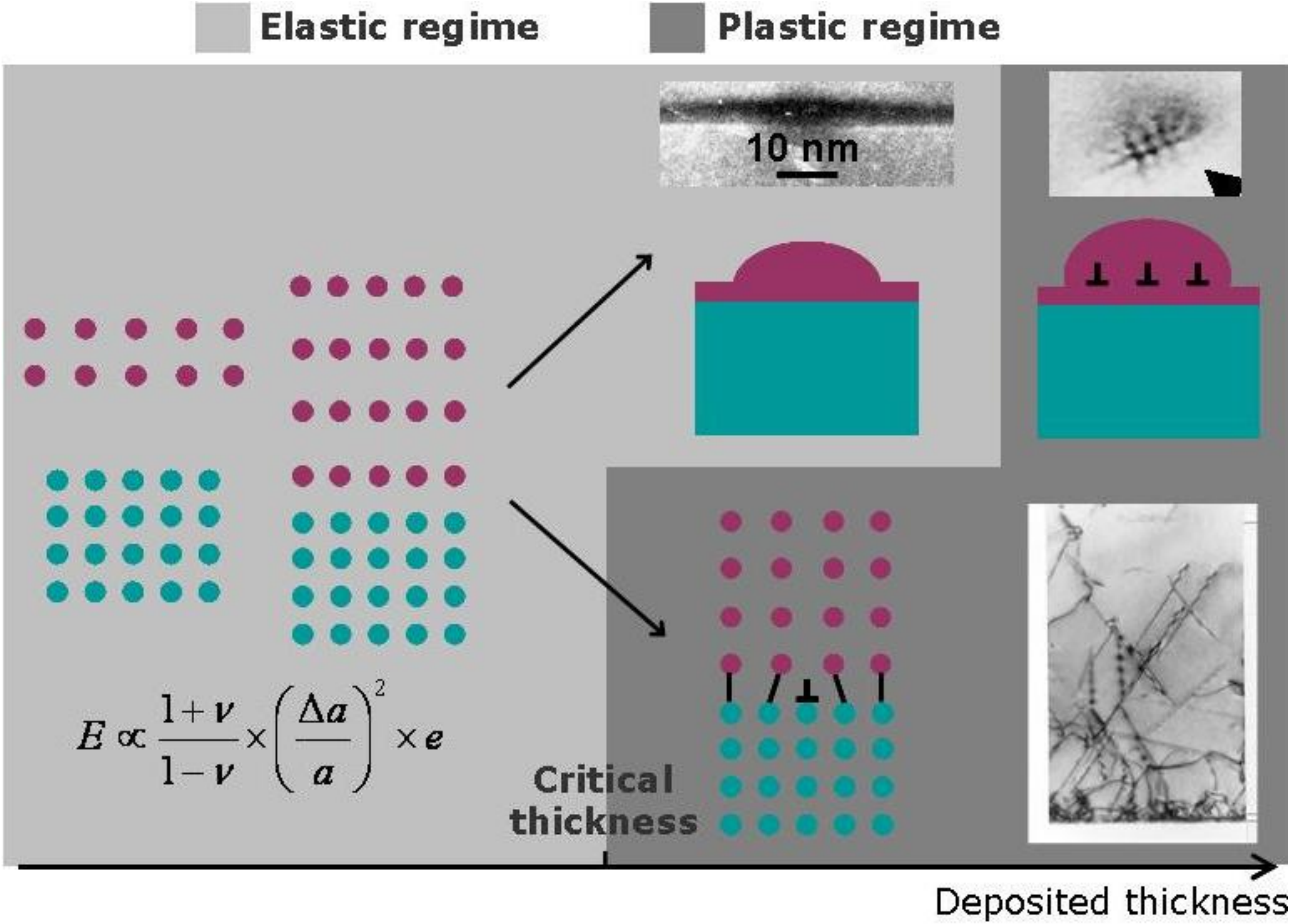

$$E \propto \frac{1+\nu}{1-\nu} \times \left(\frac{\Delta a}{a}\right)^2 \times e$$

Strained 2D growth and plastic relaxation

Dislocation mediated plastic relaxation

Critical thickness dependency to lattice mismatch

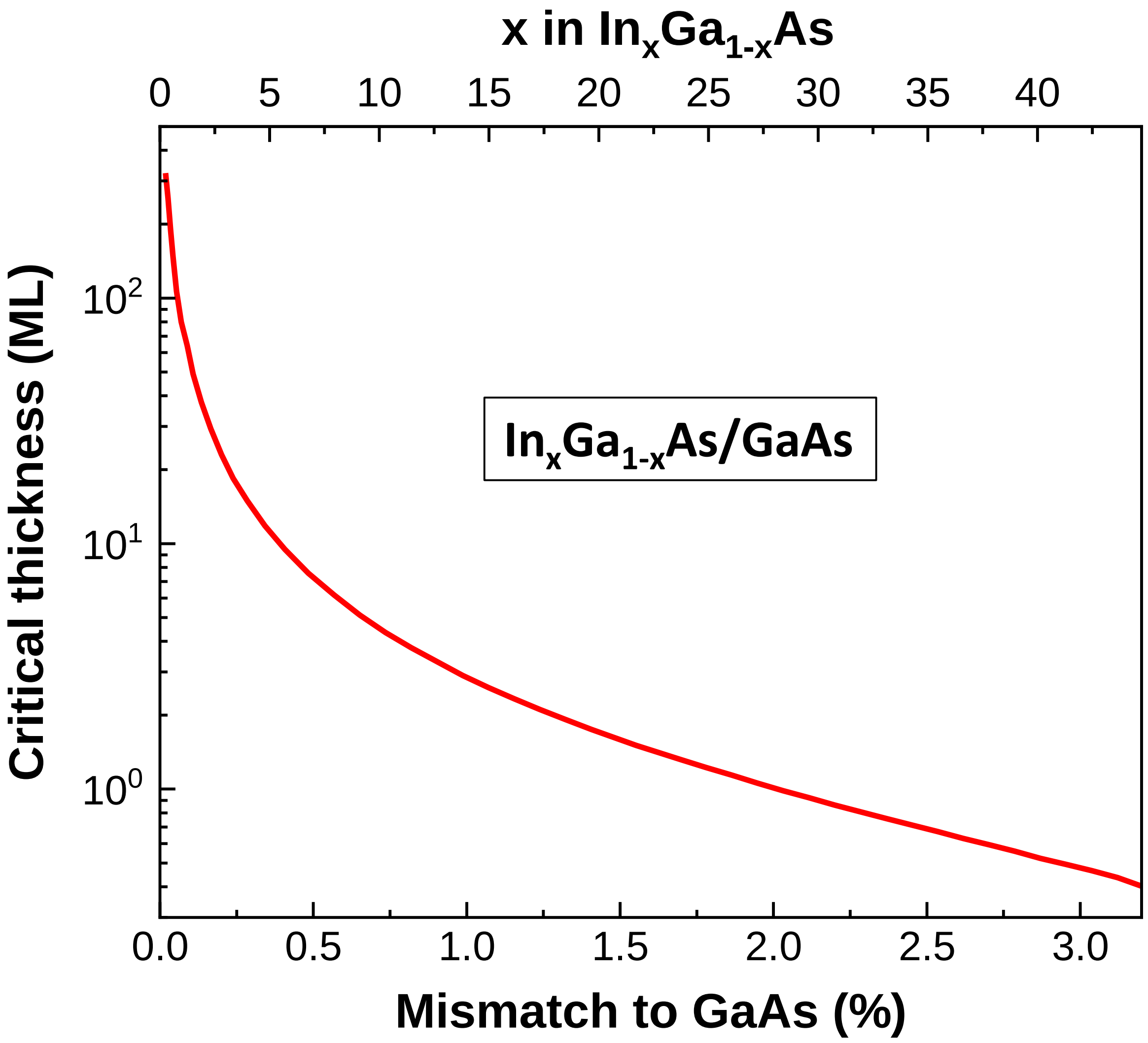

Strained 2D growth and plastic relaxation

Plastic relaxation : comparison of oxides and semiconductors

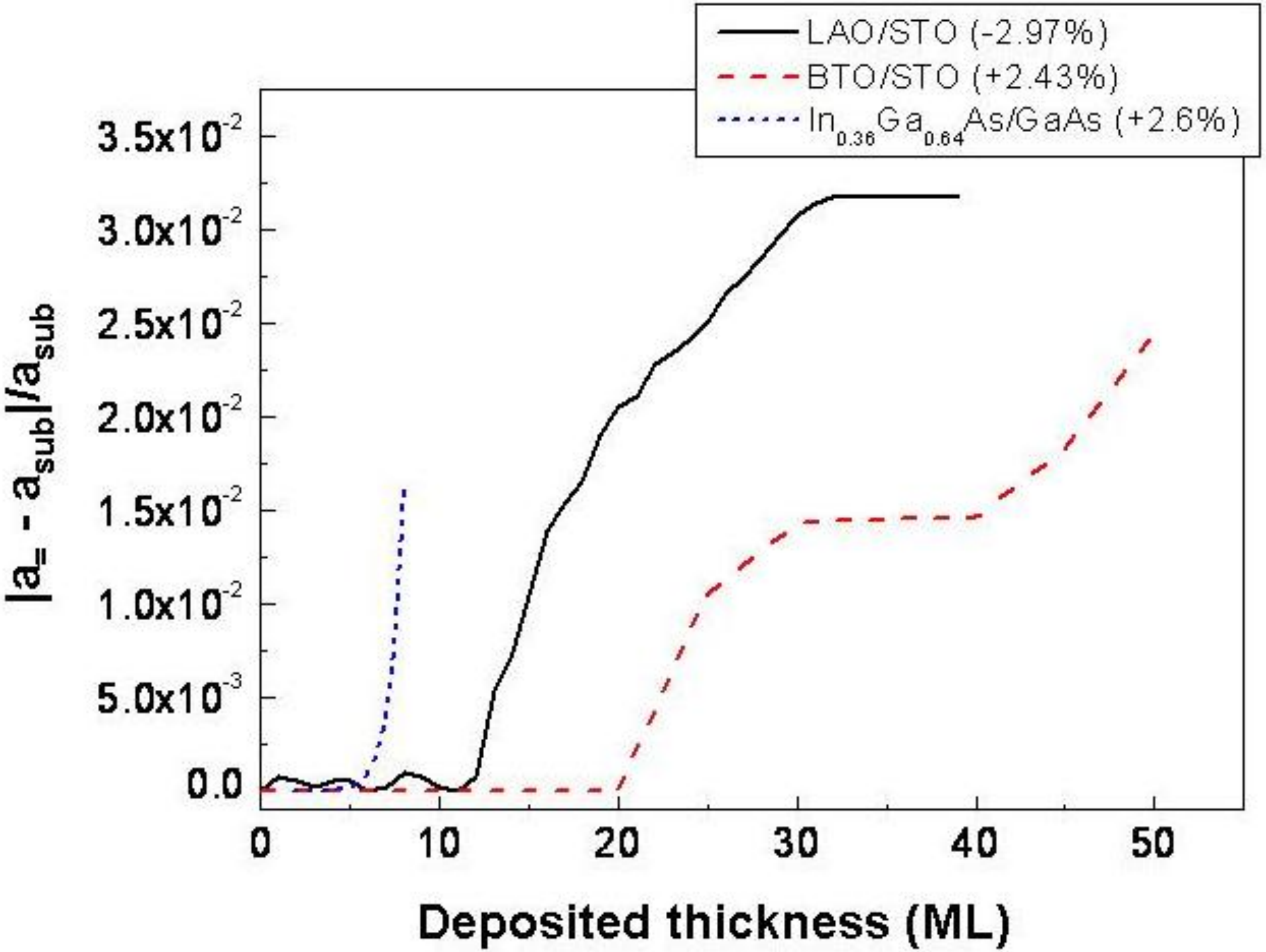

$In_{0.36}Ga_{0.54}As/GaAs$
m = 2.6%
Y ≈ 85
Polar covalent

$BaTiO_3/SrTiO_3$
m = 2.4%
Y ≈ 67
Ionic

$LaAlO_3/SrTiO_3$
m = -2.9 %
Y ≈ 331
Ionic

Strained 2D growth and plastic relaxation

Plastic relaxation : comparison of oxides and semiconductors

Zincblende
Gliding planes = {111}

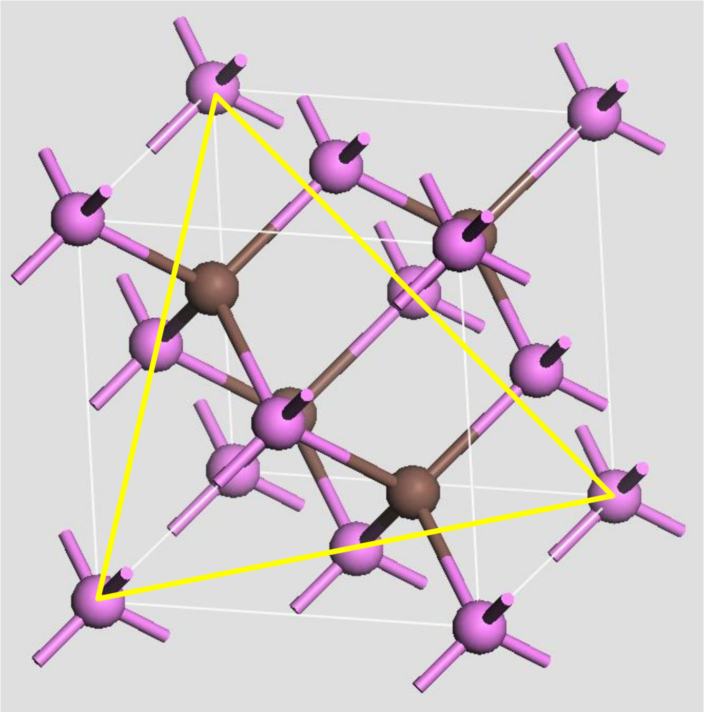

Perovskite
Gliding planes = {110}

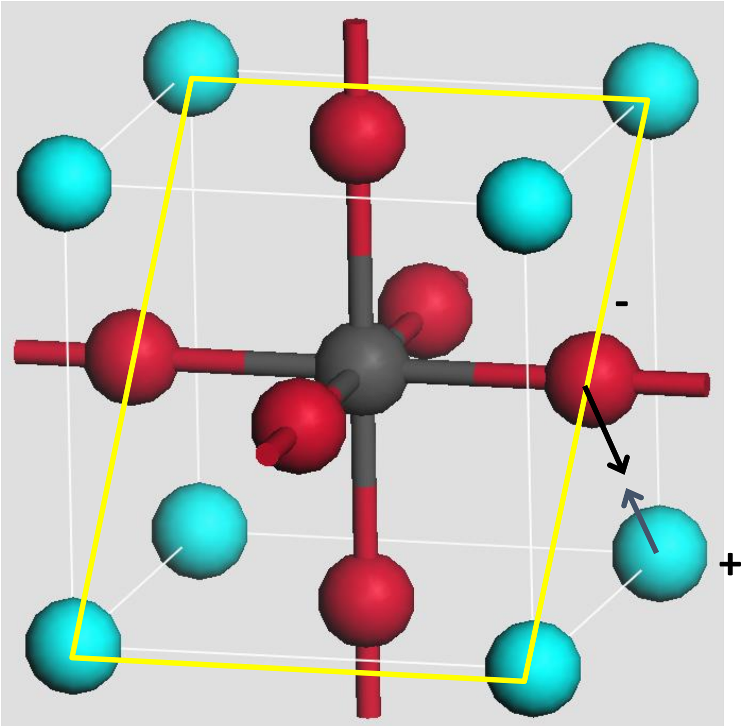

Partial charges hinder dislocation nucleation and propagation

Strained 2D growth and plastic relaxation

$BaTiO_3$ ferroelectric domain structure

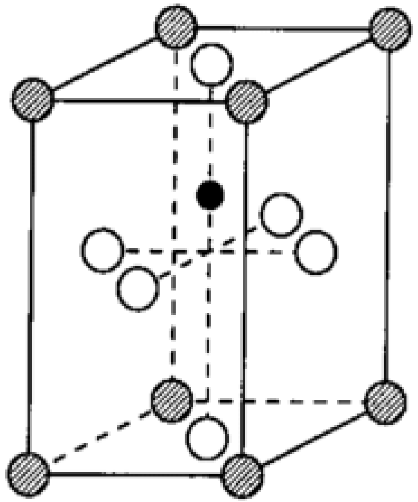

Ferroelectric axis

$r_{33} = 120\ pm/V$

$r_{42} = 500\ pm/V$

Chelladurai Nat. Mater. 2025

Optimal domain structure for non volatile memory

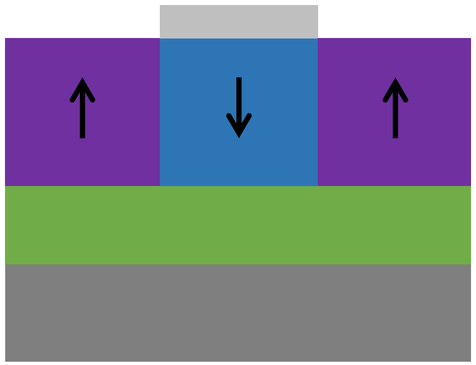

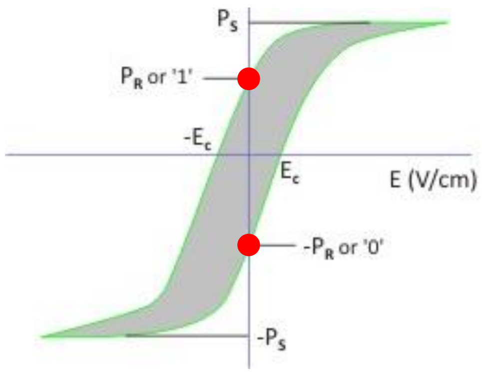

Optimal domain structure for electro-optic modulator

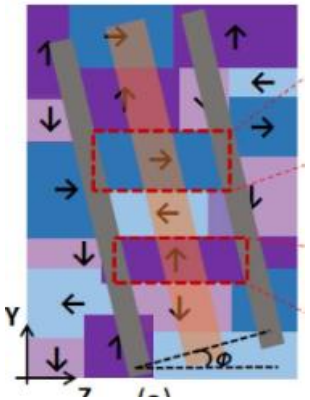

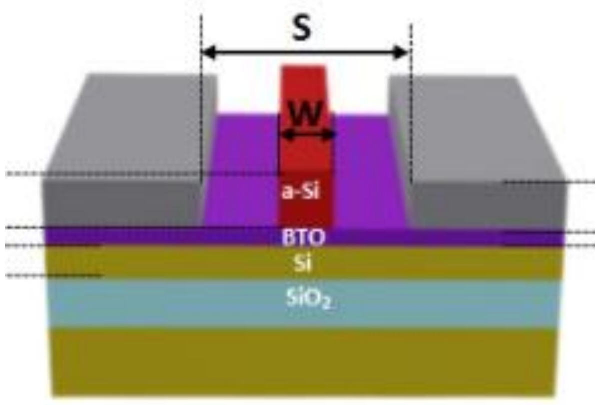

($LiNbO_3$: $r_{33} = 15\ pm/V$, $r_{33} = 30\ pm/V$)

Strained 2D growth and plastic relaxation

$BaTiO_3$ ferroelectric domain structure

@growth temperature (700°C)

@room temperature

Bulk BTO

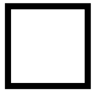

Cubic
$a_{bulk} = 4.037$ Å

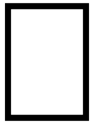

Tetragonal
$a_{bulk} = 3.992$ Å
$c_{bulk} = 4.036$ Å

BTO/STO/Si
Thin ($< \sim 30\ nm$)

Compressive epi strain

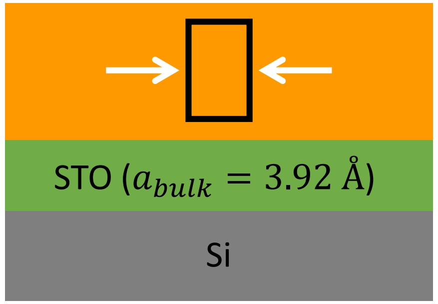

Cubic to tetragonal phase transition

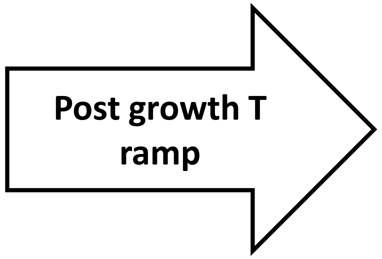

Compressive epi strain: optimal for non volatile memories

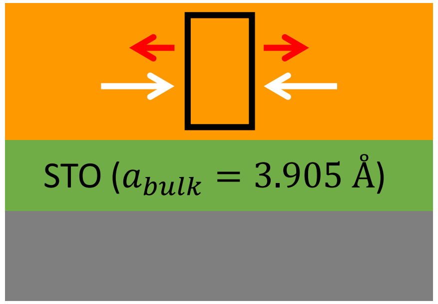

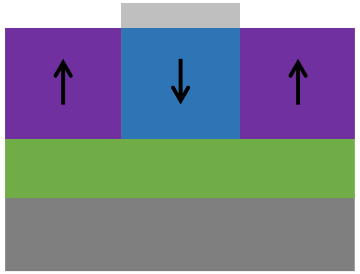

BTO/STO/Si
Thick ($> \sim 30\ nm$)

No epi strain

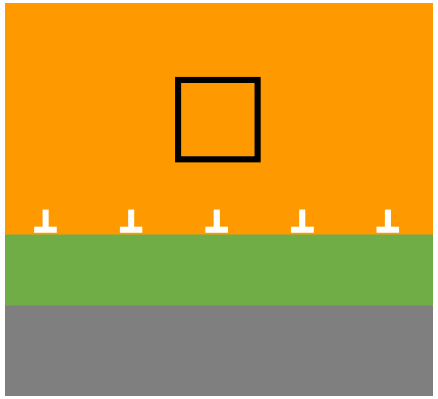

TEC
Si: $3 \times 10^{-6}\ K^{-1}$
BTO: $1.3 \times 10^{-5}\ K^{-1}$

Thermal tensile strain: optimal for electro-optic modulators

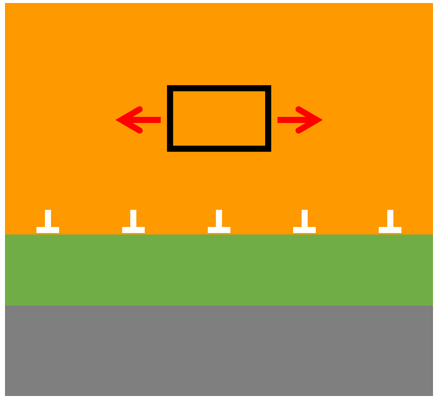

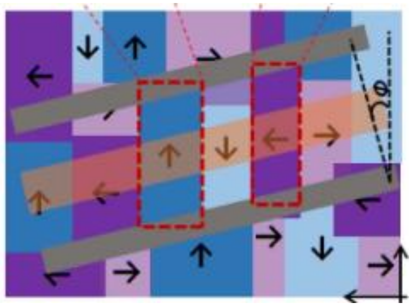

Strained 2D growth and plastic relaxation

Strain-assisted phase selection during Carpy-Gally compound growth

E. Gradauskaite et al., Adv. Mater. ***37****, 2416963 (2025)*

$SrTiO_3(110)$ substrate $LaTiO_3$: 1.4 %, $La_2Ti_2O_7$: $0.12\% \times -0.42\%$

$La_2Ti_2O_7$

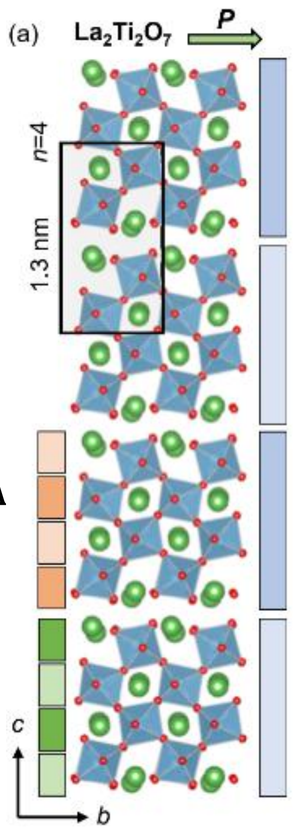

$LaTiO_3$

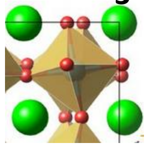

$c = 3.96$ Å

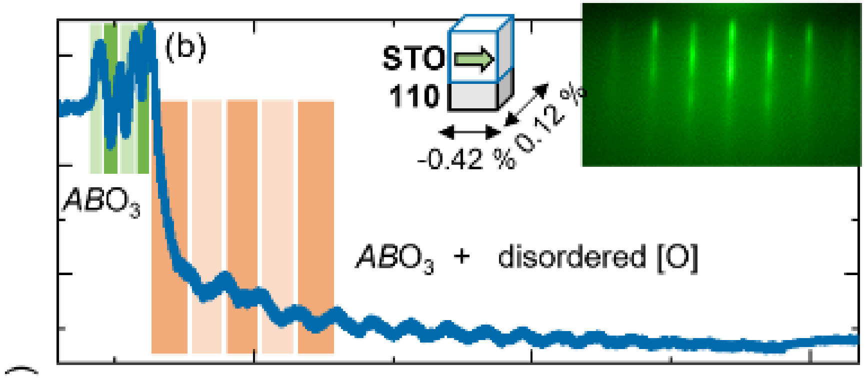

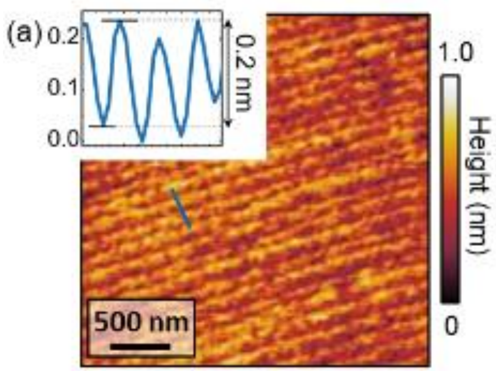

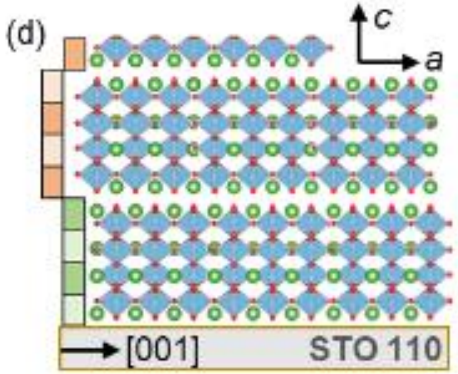

$DyScO_3(110)$ substrate $LaTiO_3$: -20%, $La_2Ti_2O_7$: $1.3\% \times 3\%$

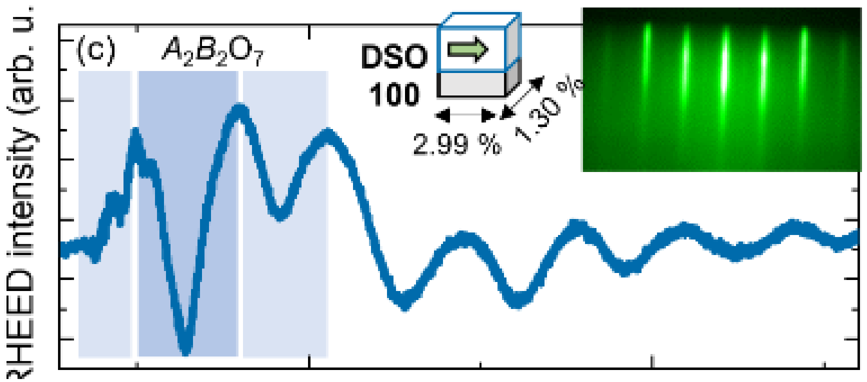

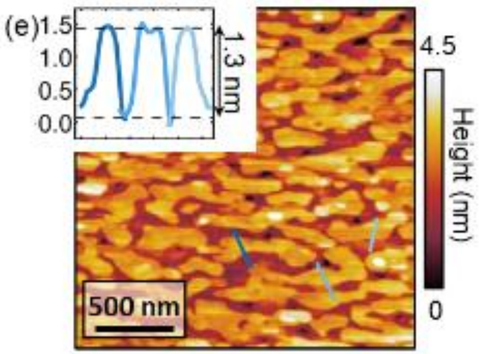

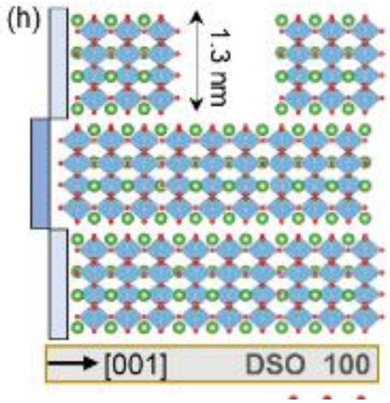

$a = 7.8$ Å
$b = 5.55$ Å
$c = 1.3\ nm$

Strain selected growth of $La_2Ti_2O_7$

Strain free 3D growth

a. Strain-induced 3D growth: Stranski-Krastanov growth mode

b. Interface induced 3D growth

Strain free 3D growth
Strain induced 3D growth

Stranski-Krastanov growth mode

InAs/GaAs
Lattice mismatch $\mathrm{m} = 7.16\%$
Strong adhesion, $\gamma_{AB} < 0$

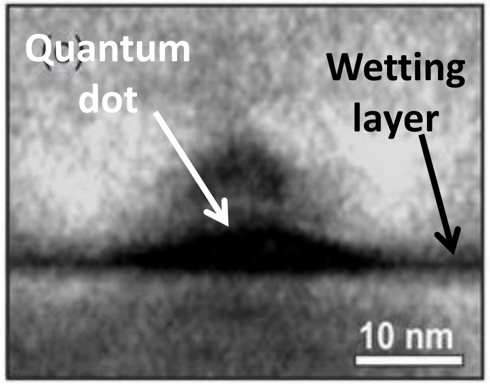

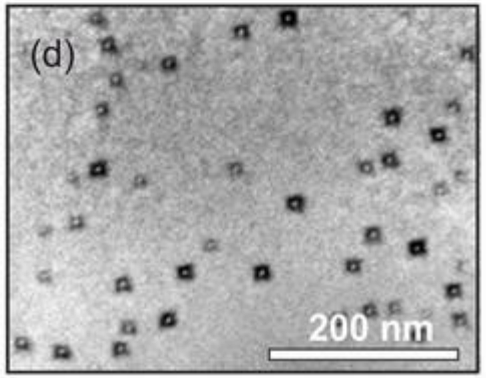

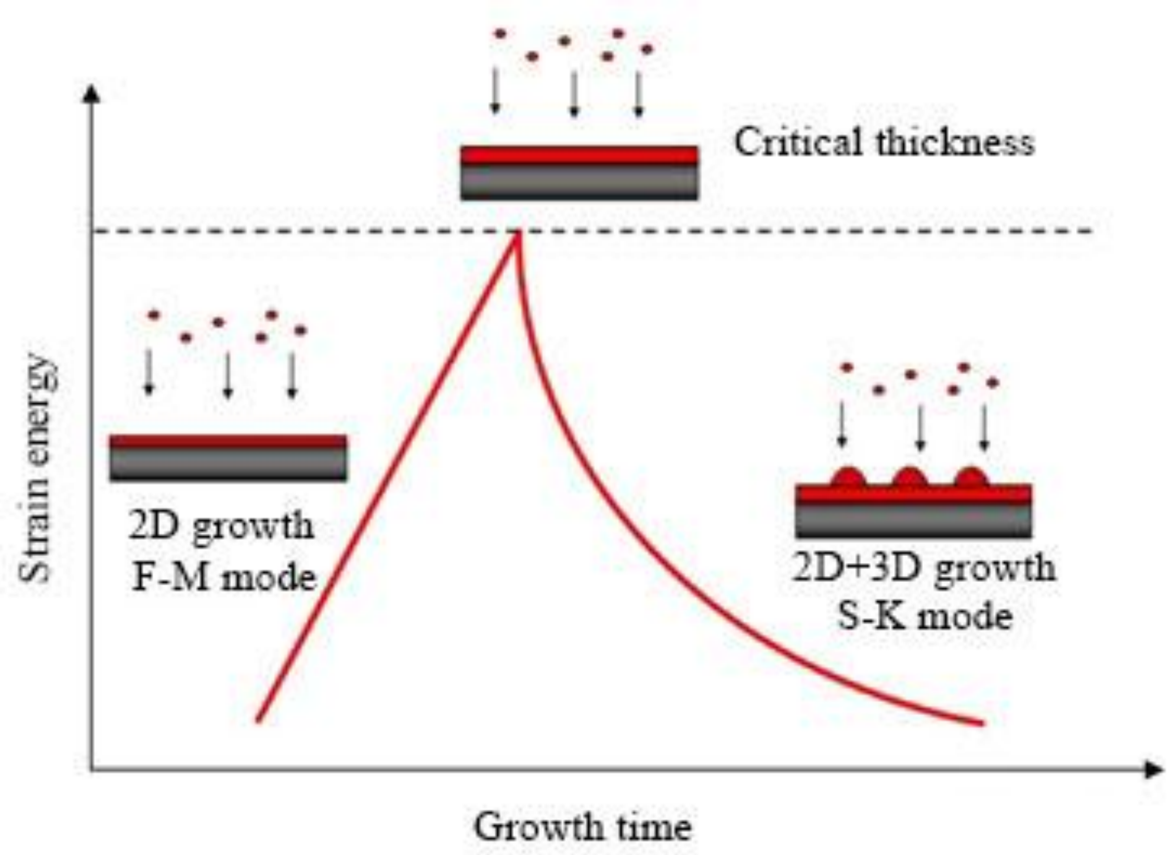

Free surface strain relaxation

Strain free 3D growth

Interface induced 3D growth

GaP/Si

*Lucci et al., Phys Rev Mat **2**, 060401(R), (2018)*

Low mismatch: $m = 0.37\%$

$\gamma_{Si} = 1.4\ J/m^2$

$\gamma_{GaP} = 0.92\ J/m^2$

$\gamma_{GaP/Si} > 0.5\ J/m^2$ (DFT)

$$\boxed{\alpha_B = \frac{\gamma_{GaP/Si} - \gamma_{Si}}{\gamma_{GaP}} > -0.98 > -1}$$

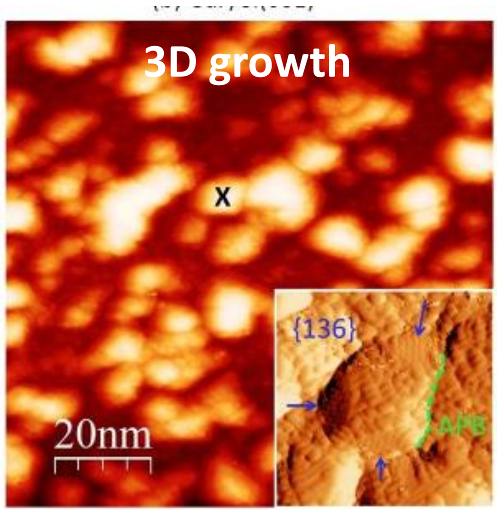

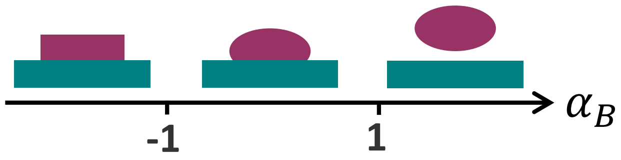

Ge/BaTiO$_3$

Low mismatch: $m = 0.2\%$

$\gamma_{BTO} = 1\ J/m^2$

$\gamma_{Ge} = 0.8\ J/m^2$

Instable Ge-O interface bonds

$$\alpha_B = \frac{\gamma_{Ge/BTO} - \gamma_{BTO}}{\gamma_{Ge}} > -1$$

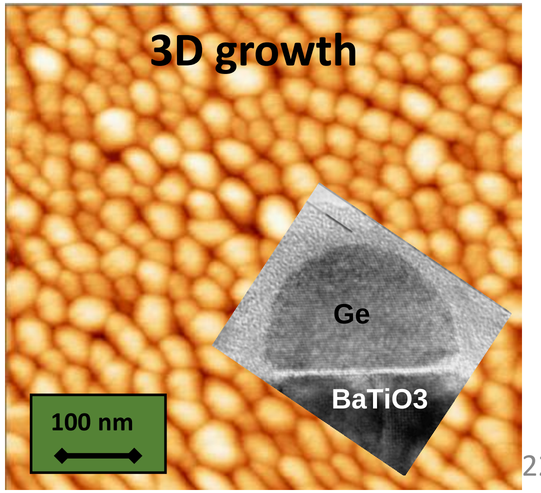

Highly dissimilar epitaxial systems

a. Indirect epitaxial relationships

- Driven by lattice mismatch
- Driven by interface energy

b. Mismatch accommodation via interfacial dislocation networks

- Dislocation entry at the early stages of the growth
- Defects formed during coalescence

b. Interface chemical reactions

- Growth window
- $SrTiO_3$/Si : the knitting machine

Highly dissimilar epitaxial systems

Indirect epitaxial relationships

$SrTiO_3$/Si(001): epitaxial relationship driven by lattice mismatch

R. McKee et al., Phys. Rev. Lett. ***81****, 3014 (1998)*

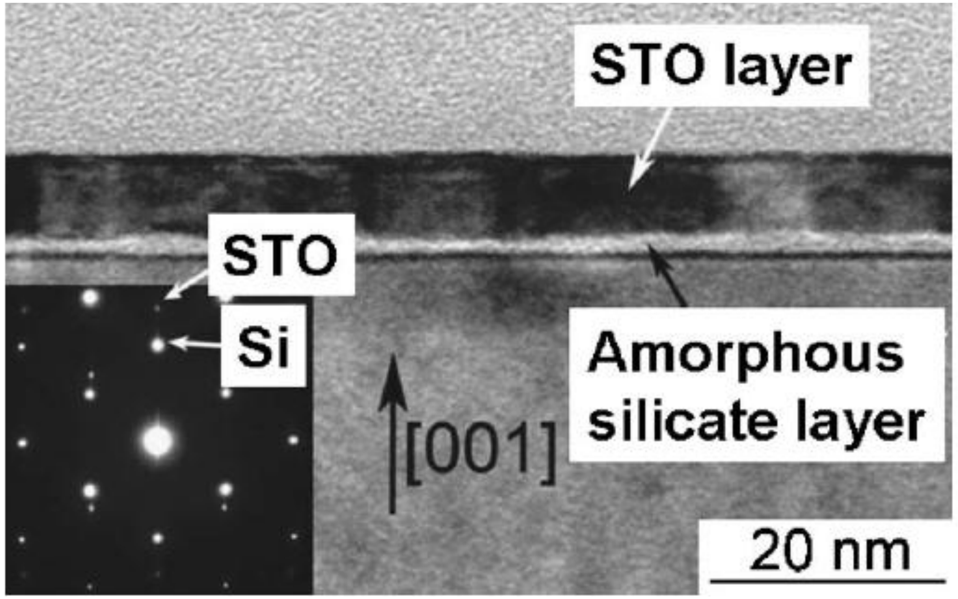

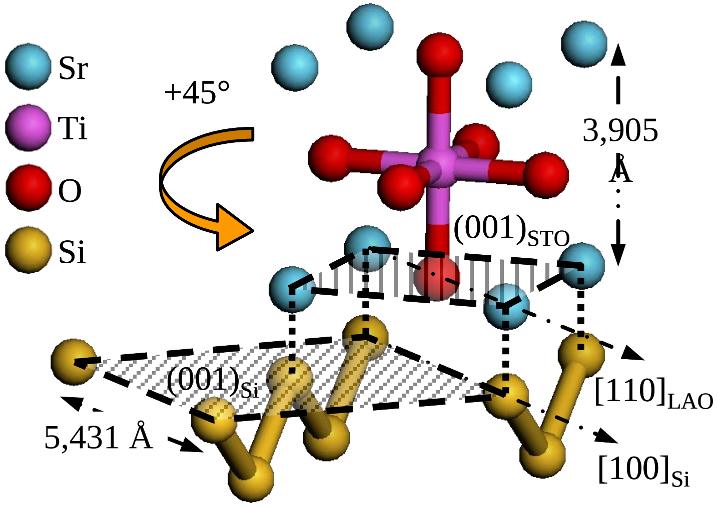

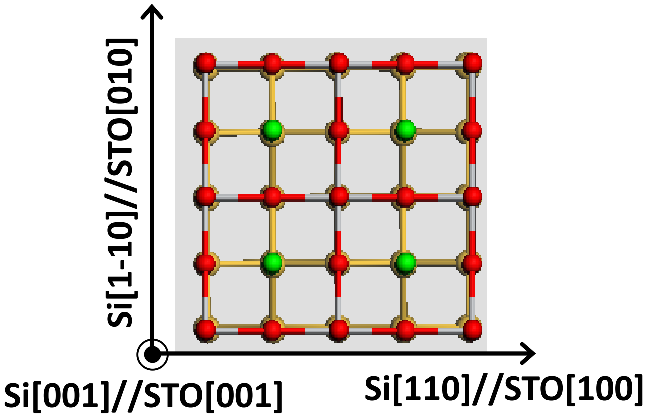

« Cube on cube »: $m = 48\%$
45° rotation: $m = 1.7\%$

Highly dissimilar epitaxial systems
Indirect epitaxial relationships

Gd_2O_3/Si(001): epitaxial relationship driven by interface energy

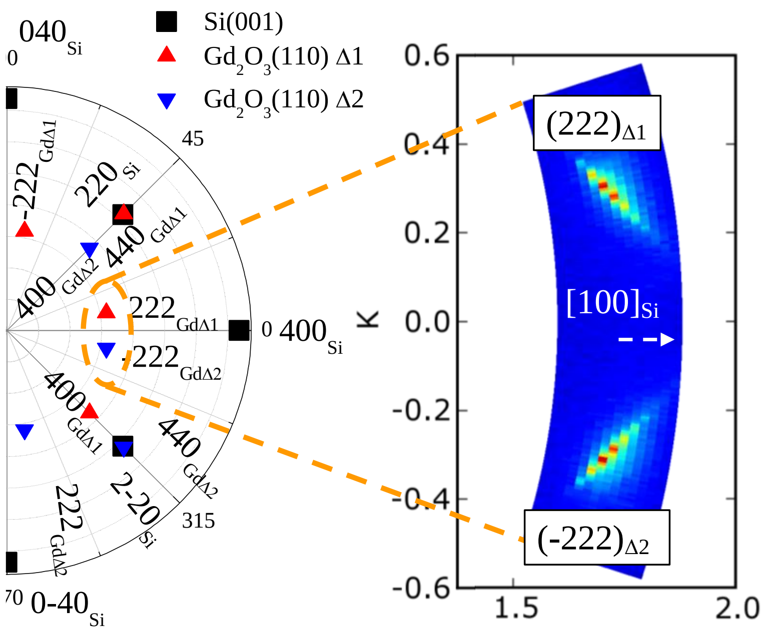

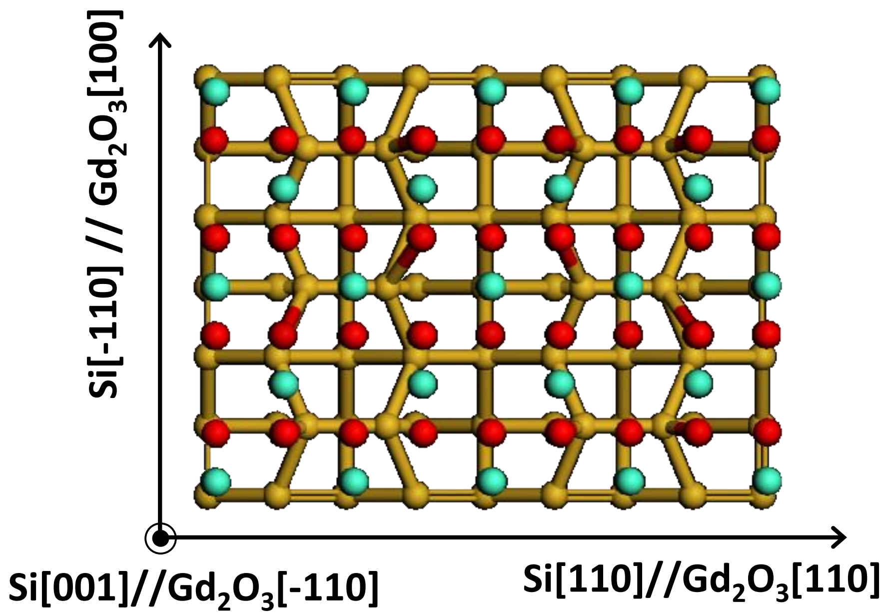

« Cube on cube »: $m = -0.44\%$, $\mathbf{62\%}$ **dangling bonds**
Indirect: $m = -0.44 \times 5.6\%$, $\mathbf{25\%}$ **dangling bonds**

Osten et al., Phys. Status Solidi (a), ***205****, 695 (2008)*

Highly dissimilar epitaxial systems

Mismatch accommodation via interfacial dislocation networks

InP/$SrTiO_3$ and Ge/$SrTiO_3$

Danescu et al., Appl. Phys. Lett. ***103****, 021602 (2013), Saint-Girons et al., Appl. Phys. Lett.* ***92****, 241907 (2008)*

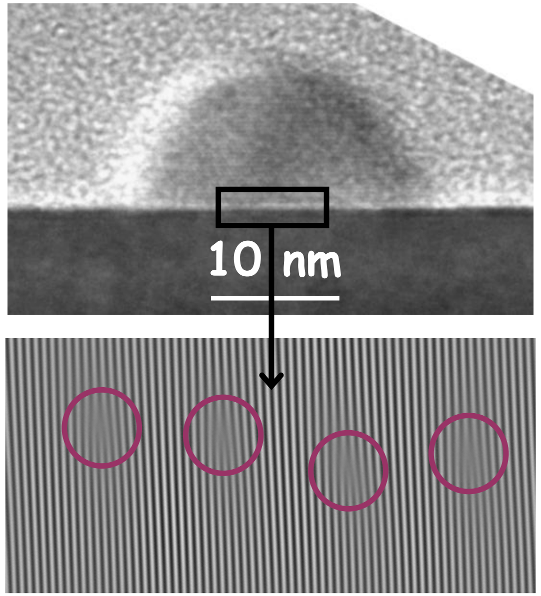

Indirect epitaxial relationship

<110>InP(001)//<100>STO(001)

Da/a = 6.3%

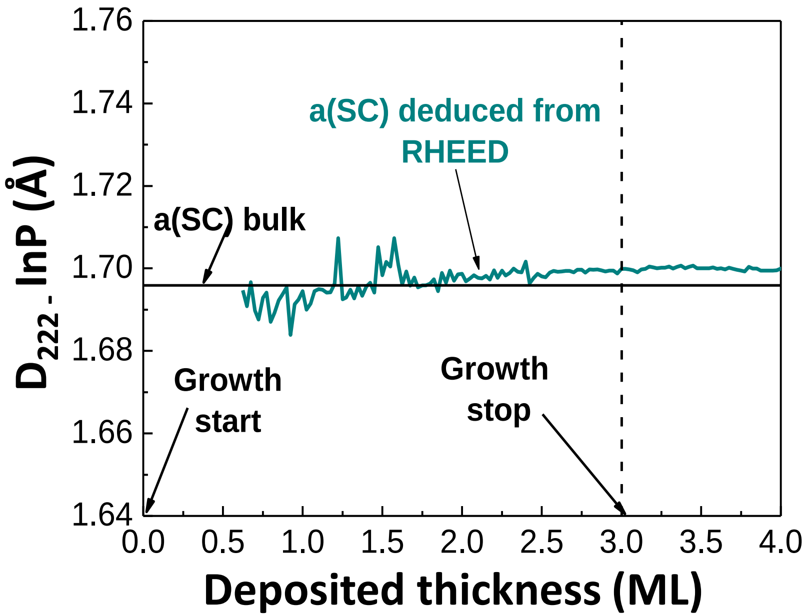

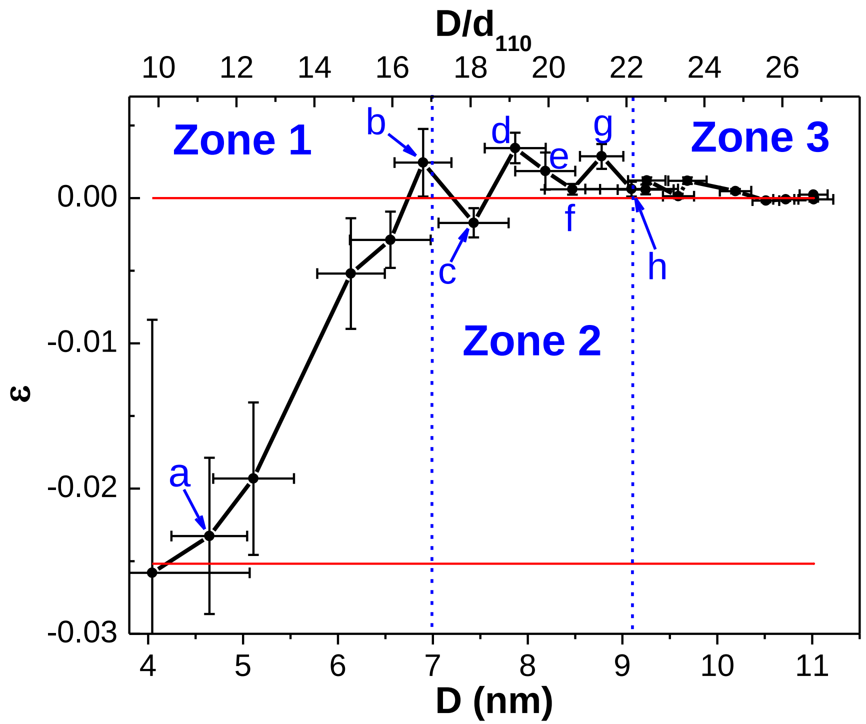

Full mismatch accommodation by interface dislocations formed at the very early stages of the growth

Highly dissimilar epitaxial systems

Mismatch accommodation via interfacial dislocation networks

InP/$SrTiO_3$: coalescence

Step 1
islands

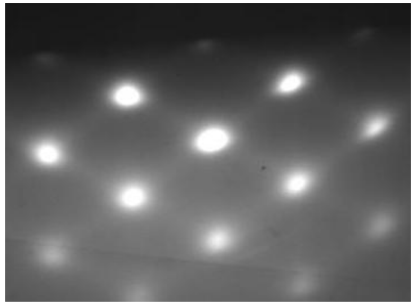

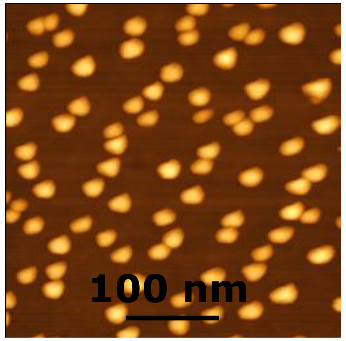

Low temperature (400°C)
High P (10^{-5} Torr)
➔ **condensation**

Step 2
coalescence

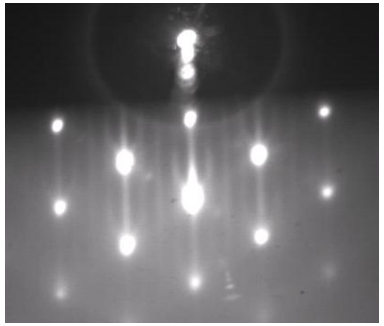

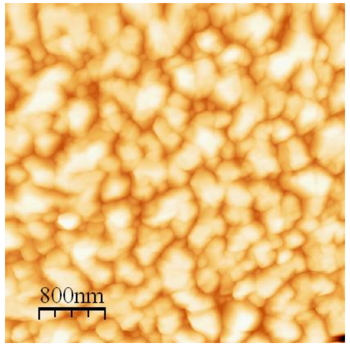

High temperature (510°C)
Low P (10^{-6} Torr)
➔ **Surface diffusion**

Step 3
growth

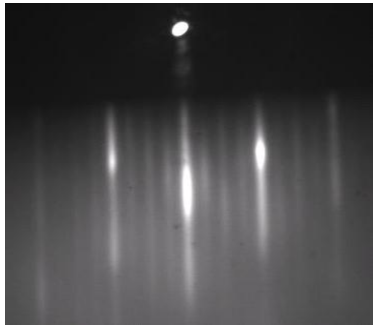

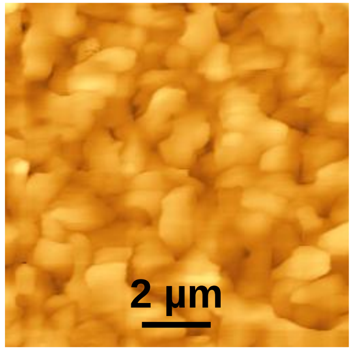

480°C – 10^{-5} Torr
➔**Standard InP conditions**

Highly dissimilar epitaxial systems

Mismatch accommodation via interfacial dislocation networks

Integration of InP based heterostructures on Si using $SrTiO_3$ templates

500 nm thick InAsP/InP/STO/Si quantum well heterostructure

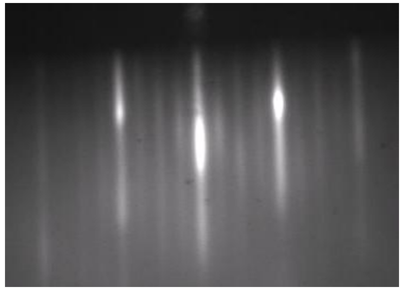

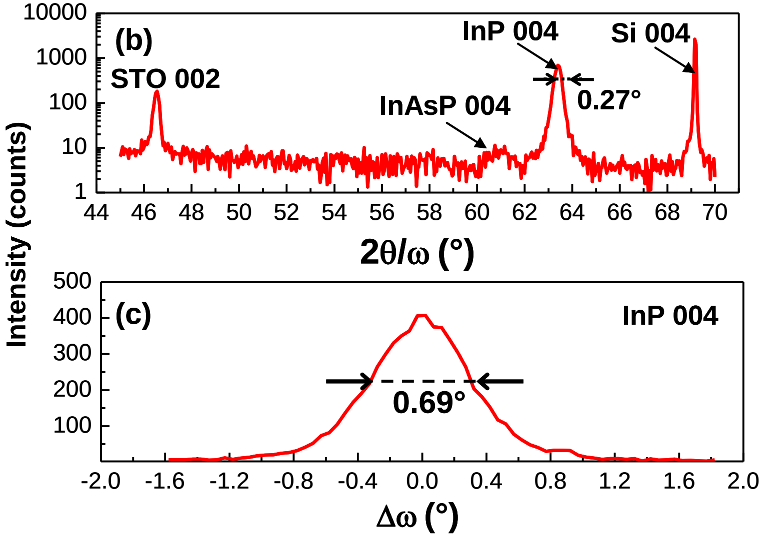

Gobaut et al, Appl. Phys. Lett. ***97****, 201908, (2010)*

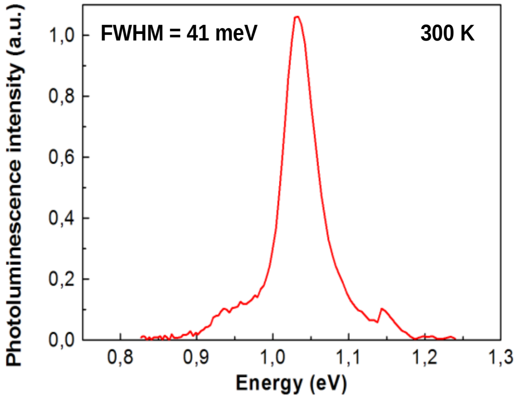

Intense and narrow PL signal @300K

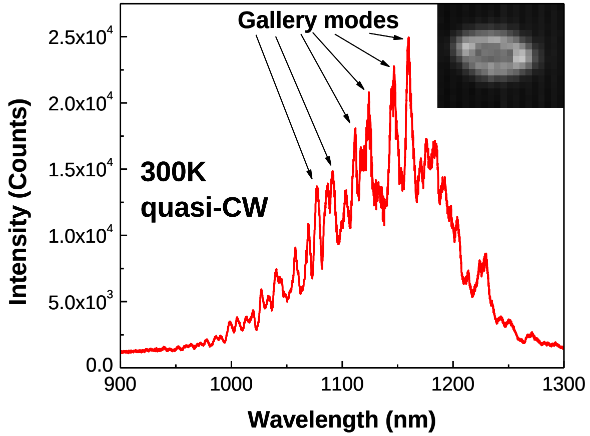

Microdisk laser : light amplification but no lasing

Highly dissimilar epitaxial systems

Mismatch accommodation via interfacial dislocation networks

Integration of InP based heterostructures on Si using $SrTiO_3$ templates: defects and limitations

InP orientation depends on growth conditions

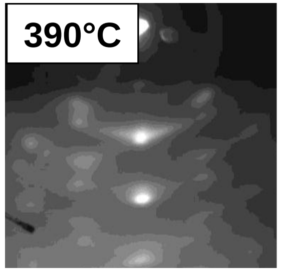

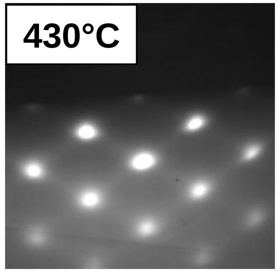

InP(111) / STO(001)   InP(001) / STO(001)

Twins are formed due to strong InP dewetting

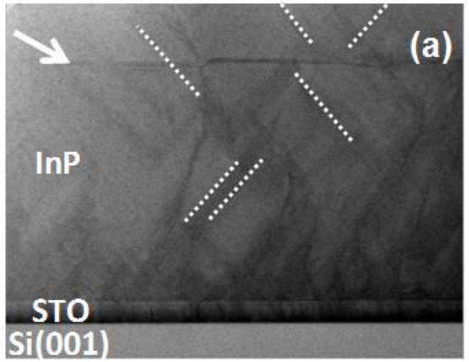

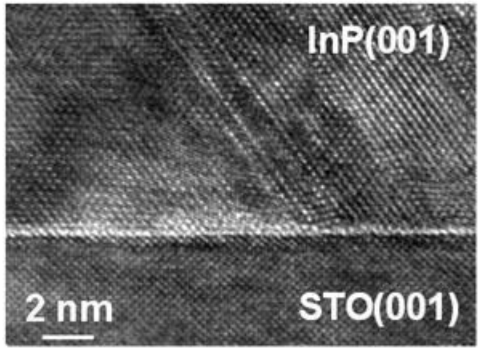

Antiphase Domains

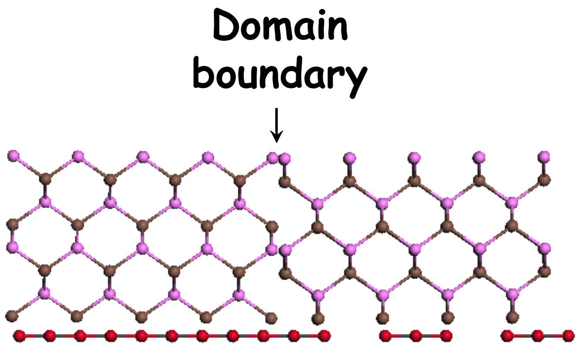

Commensurability and interface dislocation network

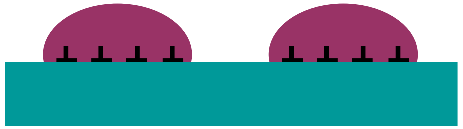

There is no reason why lateral registry between neighbouring islands should be maintained

➔ **Defect formation during coalescence**

Highly dissimilar epitaxial systems

Interface chemical reactions

Growth window: Gd_2O_3/Si(111)

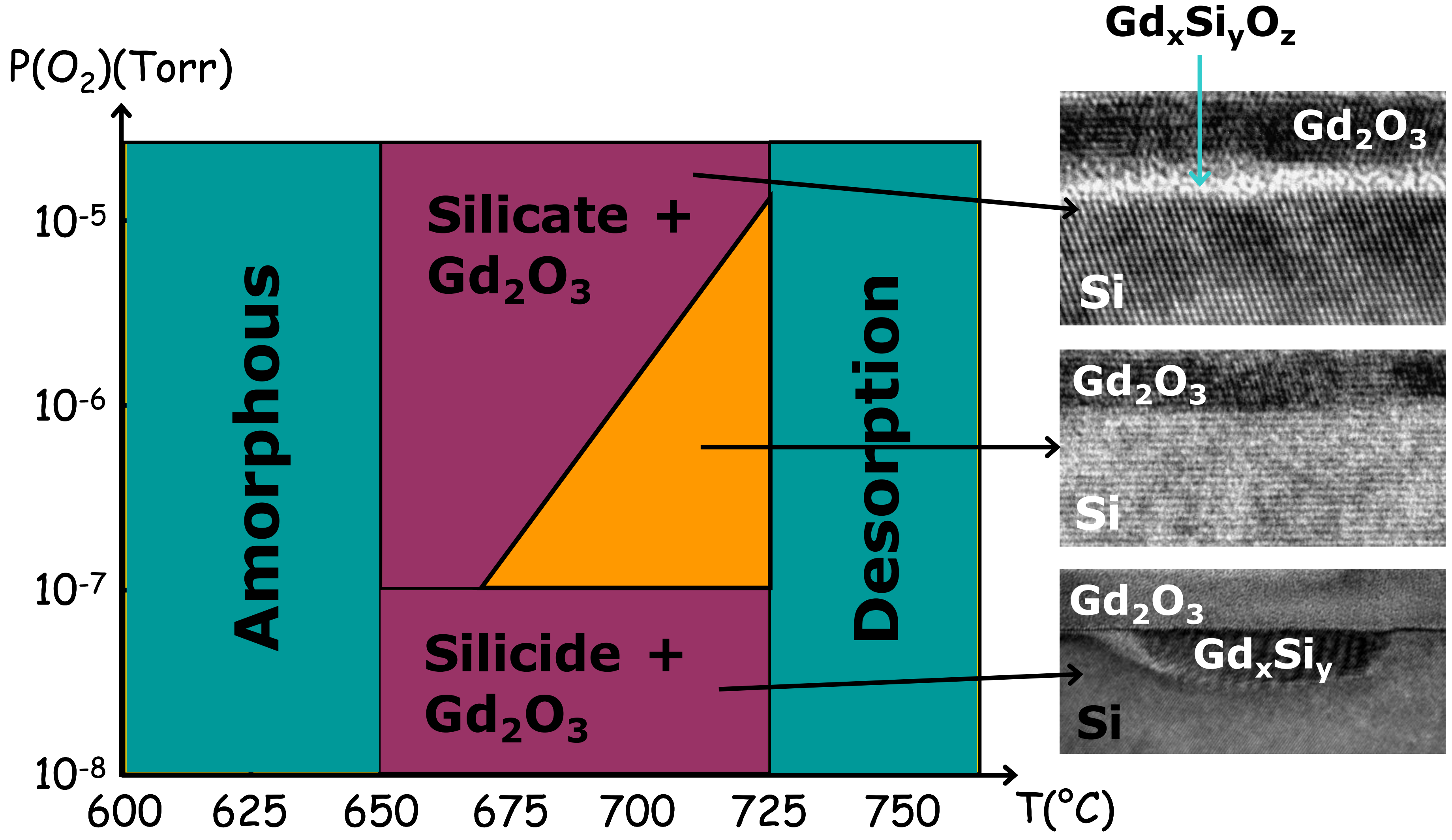

Highly dissimilar epitaxial systems
Interface chemical reactions

Growth window: $SrTiO_3$/Si(001)

The direct growth of $SrTiO_3$ on Si is impossible : silicates/silicides formation

➔ Si surface passivation

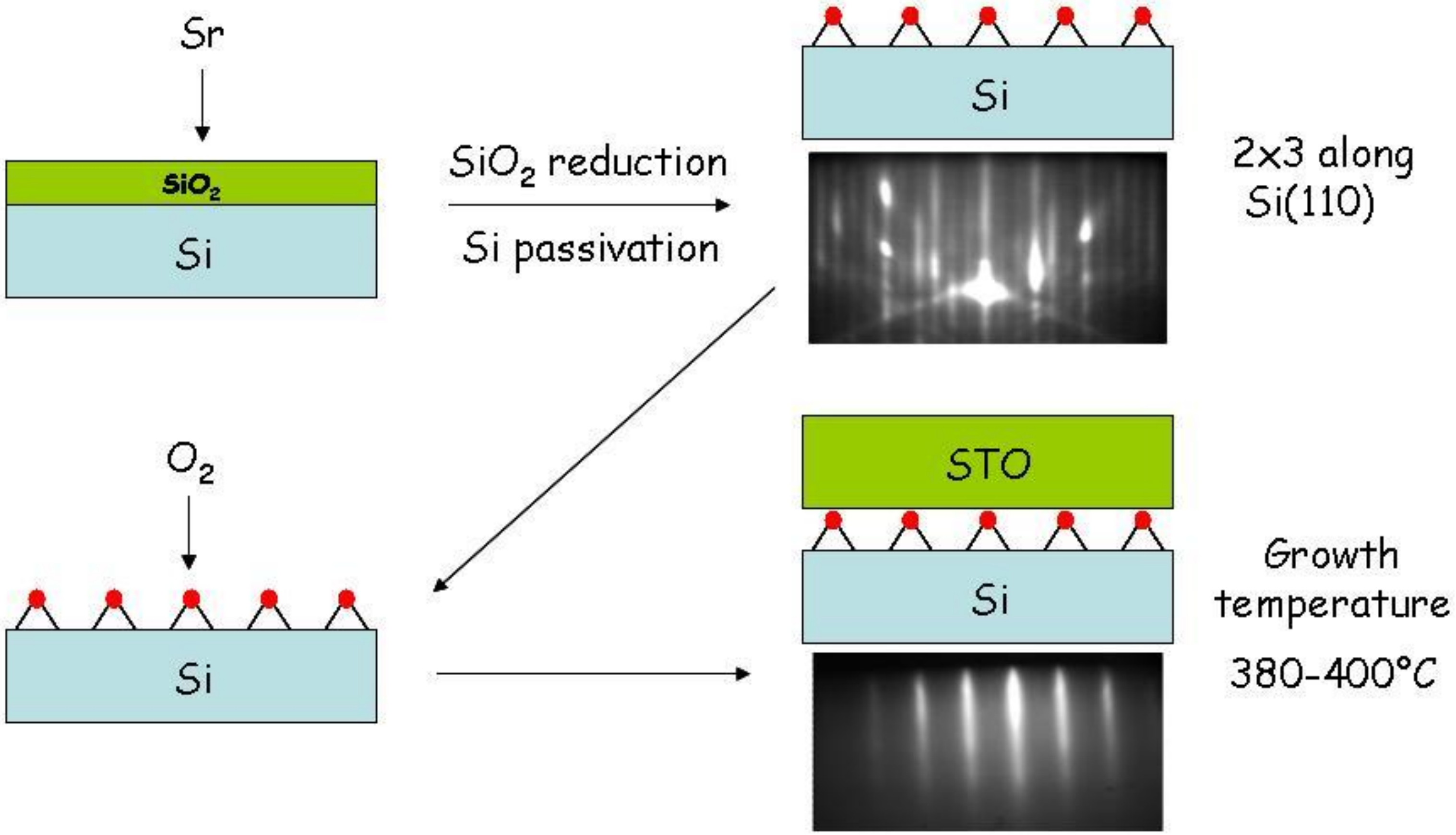

Highly dissimilar epitaxial systems

Interface chemical reactions

Growth window: $SrTiO_3/Si(001)$

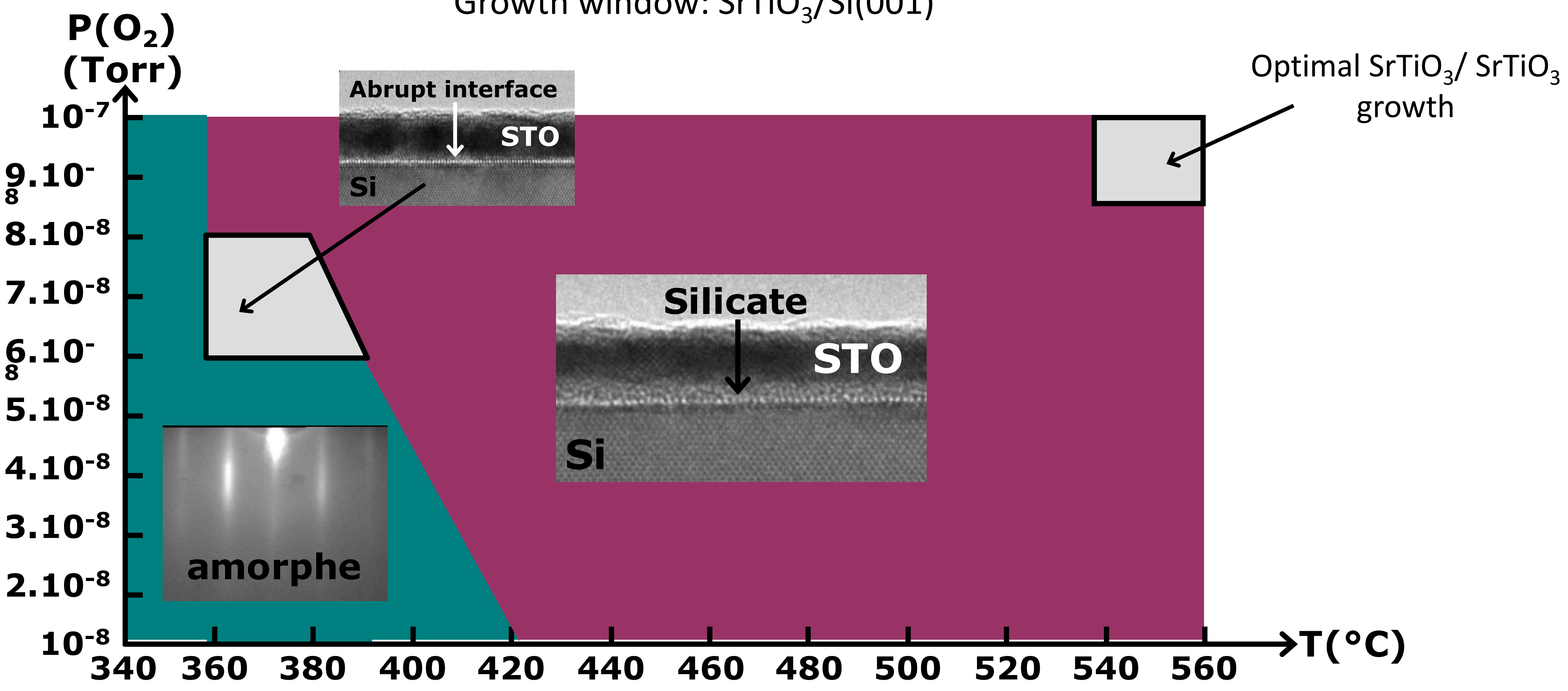

Narrow growth window

Highly dissimilar epitaxial systems

Interface chemical reactions

$SrTiO_3$/Si(001): crystallization process

Saint-Girons et al., Chem. Mat. ***28****, 5347 (2016)*

RHEED

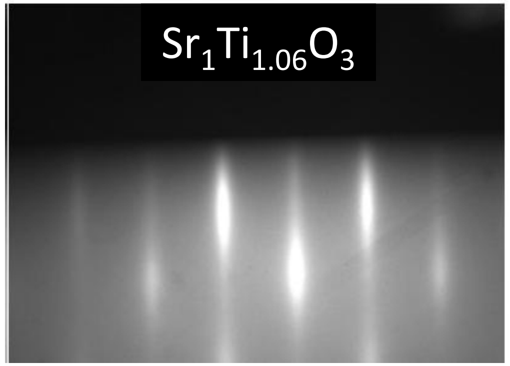

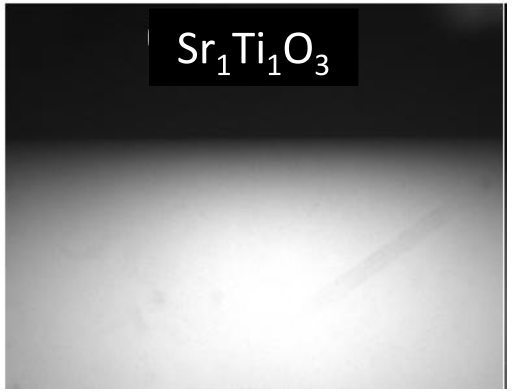

XRD

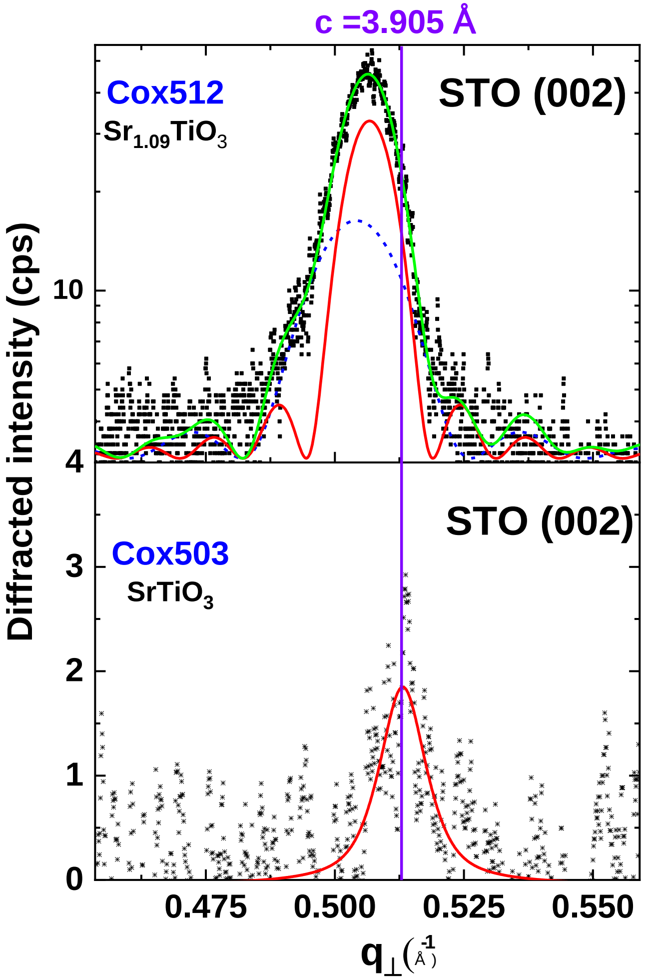

$SrTiO_3$ growth process :

1-deposition of (partially) amorphous STO @300°C

2-crystallization by annealing @450°C under UHV

$SrTiO_3$ crystallization requires an excess of Sr

Highly dissimilar epitaxial systems

Interface chemical reactions

$SrTiO_3$/Si(001): crystallization process

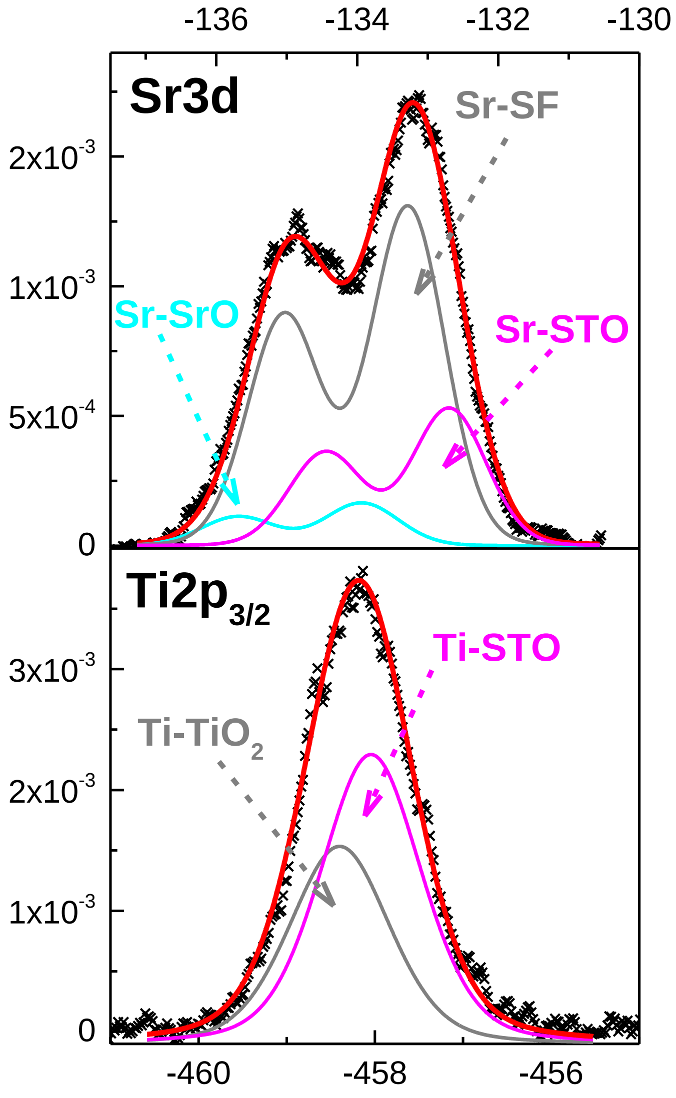

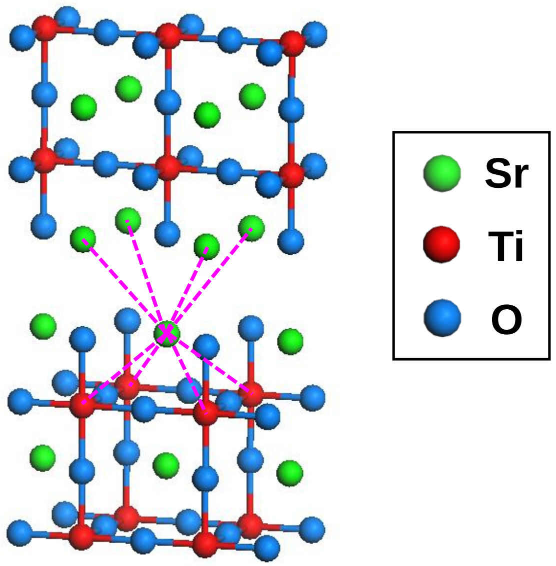

Order parameter P (P=1 for pure STO)

$$P = \frac{n(Sr-Ti) - (n(Sr-Sr) + n(Ti-Ti))}{n(Sr-Ti) + n(Sr-Sr) + n(Ti-Ti)}$$

« STO » is composed of
STO, SF, SrO and TiO_2 ~ **partial demixion**

Highly dissimilar epitaxial systems

Interface chemical reactions

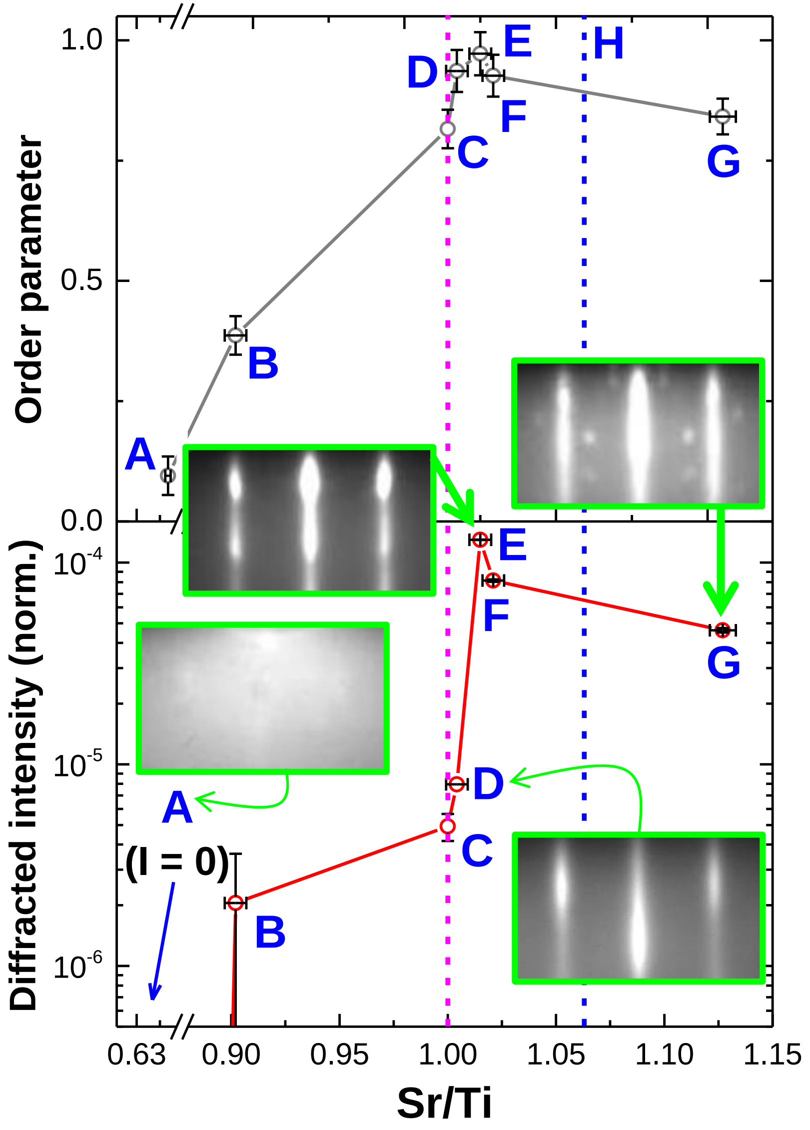

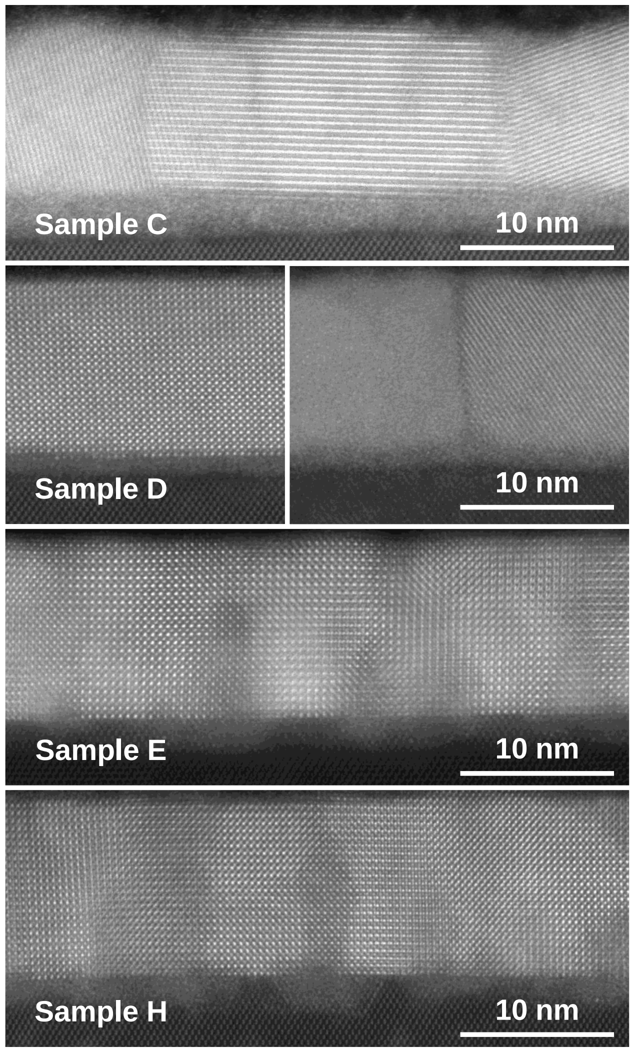

Sr/Ti = 1.015: optimal chemical and structural order

Highly dissimilar epitaxial systems
Interface chemical reactions

$SrTiO_3$/Si(001): crystallization process

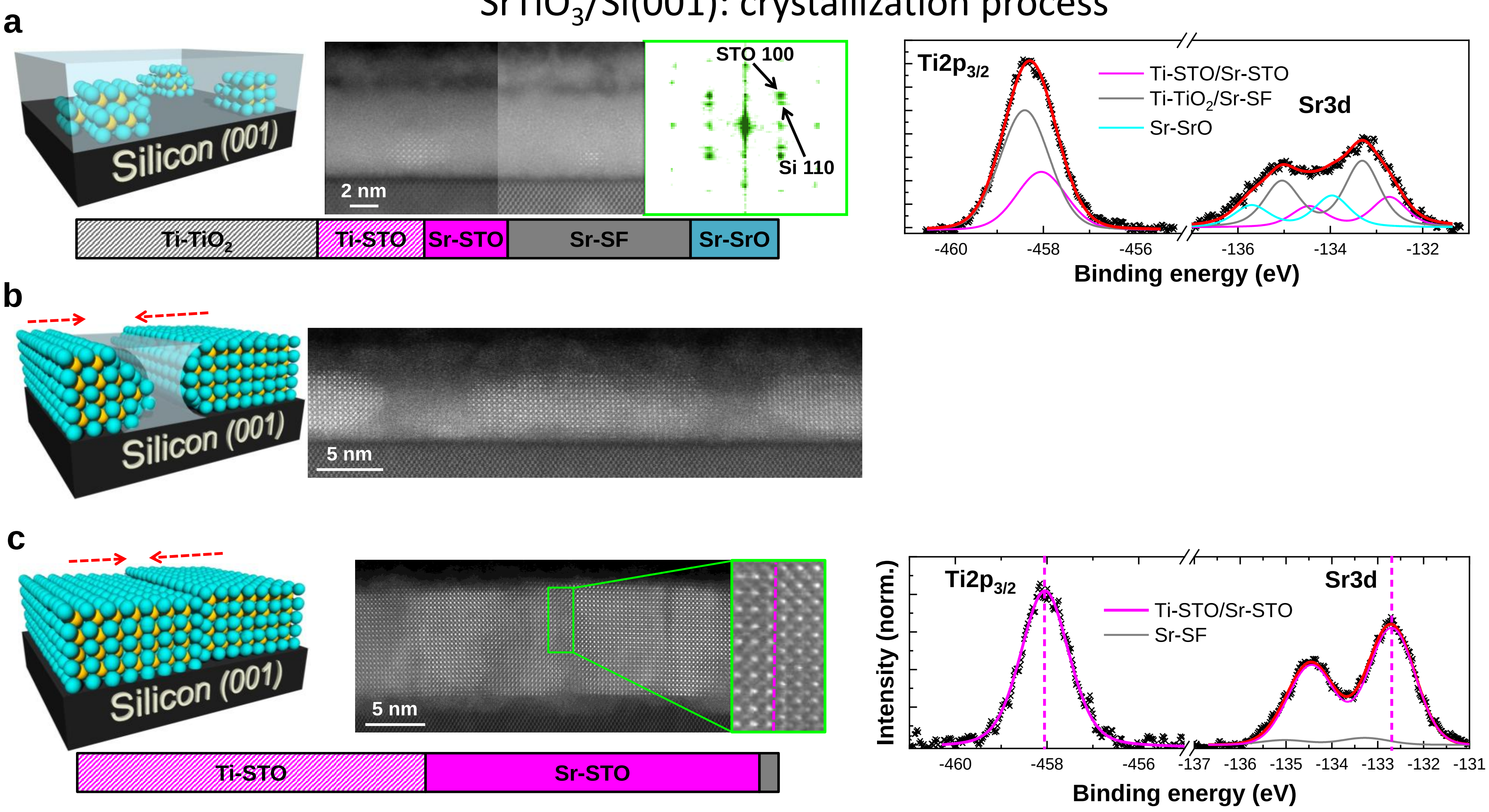

- **Cristallization = propagation of a Sr-rich front**
- **SF are formed when neighboring cristallites coalesce**

Highly dissimilar epitaxial systems

Interface chemical reactions

$SrTiO_3$/Si(001): crystallization process

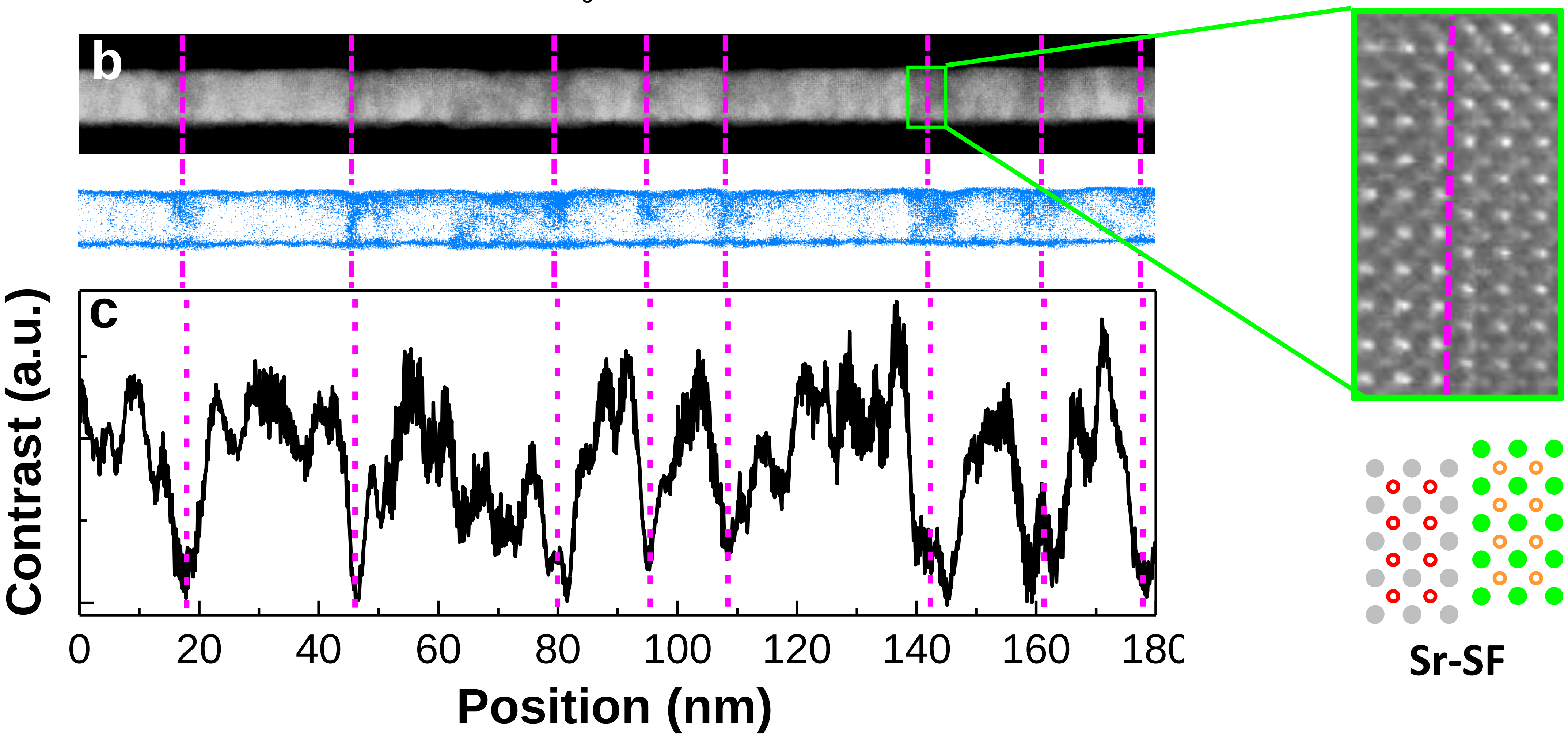

After crystallization: antiphase domain morphology

Conclusion and future challenges

a. Oxide/Si templates: a mature integration technology

b. MBE for oxide growth: advantages and challenges

Conclusion and future challenges

Oxide/Si templates: a mature integration technology

$SrTiO_3$/Si : good structural quality can be achieved

Wang Phys. Rev. Mat. ***3****, 073403 (2019)*

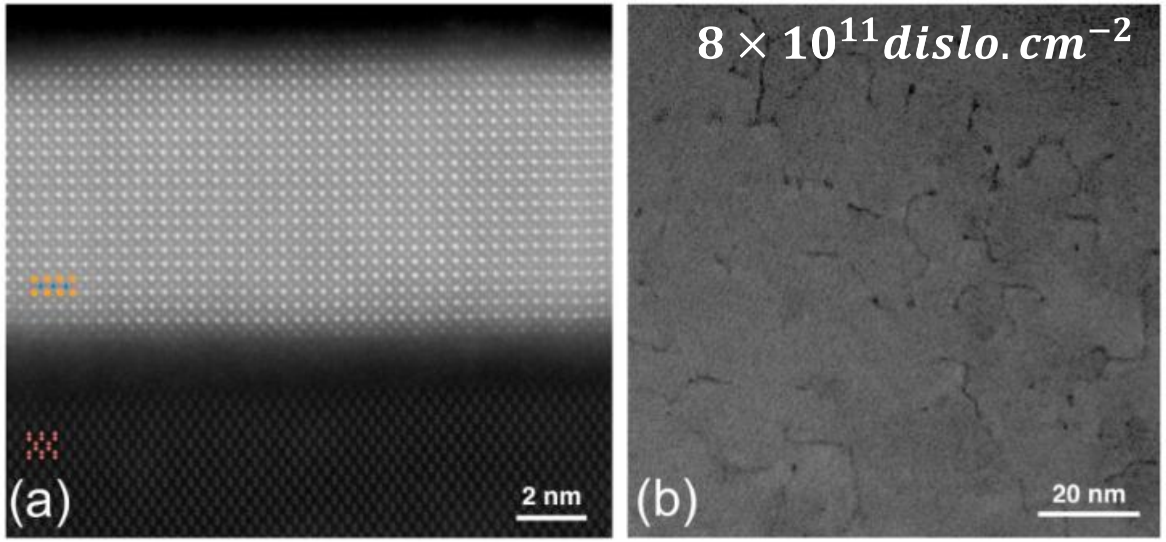

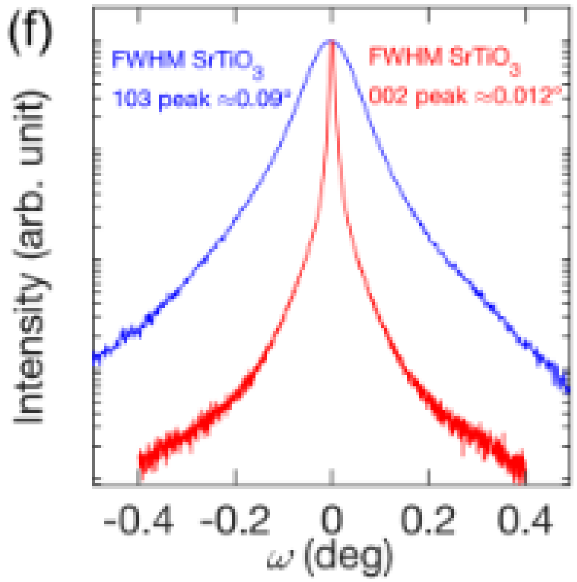

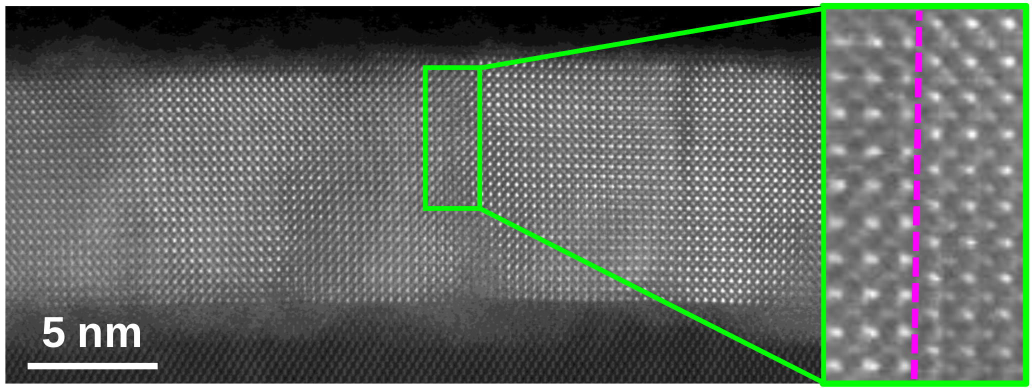

Dislocations and out-of-plane antiphase boundaries resulting from the crystallization process limit the structural quality

Conclusion and future challenges

Oxide/Si templates: a mature integration technology

A short review

- TiO_2 → photocatalytic water splitting
  Choi J. Appl. Phys. ***111***, *064112, (2012)*
- $LaCoO_3$ → thermoelectric, ferromagnetic
  Posadas Appl. Phys. Lett. ***98***, *053104, (2011)*
- $BaTiO_3$ → nanoelectronic/memories/photonics
  Niu Microelec. Eng. ***88***, *1232, (2011)*
  Dubourdieu Nature Nanotech. ***8***, *881, (2013)*
  Scigaj Appl. Phys. Lett. ***109***, *122903 (2016)*
  Eltes J. Ligthw. Tec. ***37***, *1456 (2019)*
- $LaAlO_3$ → high-k dielectric
  Mi Appl. Phys. Lett. ***90***, *181925, (2007)*
- $BiFeO_3$ → multiferroic
  Wang Appl. Phys. Lett. ***85***, *2574, (2004)*
- PZT → RF-filters/MEMS
  Lin Appl. Phys. Lett. ***78***, *2034, (2001)*
- $LaSrMnO_3$ → **spintronics, sensors**
  Le Bourdais J. Appl. Phys. ***118***, *124509, (2015)*
- ***PMN-PT*** → **RF-filters/MEMS**
  Baek Science ***334***, *6058 (2011)*
- ***Diamond*** → **high power electronics**
  Arnault Diamond Rel. Mat. ***105***, *107768 (2020)*
- ***$HfZrO_2$*** → **nanoelectronics**
  Song Nanoscale ***15,*** *222901 (2023)*
- ***LiNbO3*** → **photonics**
  Bartasyte, Nanotechnology ***35***, *(2024)*
- ***$Li_4Ti_5O_{12}$*** → **batteries**
  Lacey, ACS Applied Mat. Int. ***15***, *1535 (2022)*
- ***…***

Lumiphase

Commercial BTO/STO/Si electro-optic modulator

Conclusion and future challenges

MBE for oxide growth: advantages and challenges

MBE presents unique features for oxide growth

- Flexible composition control
- Interface engineering ➔ oxide/semiconductor integration
- Heterostructures and superlattices
- High structural quality

Reproducible composition control under oxygen remains challenging

- Source drift due to elemental load oxidation
- Flux measurement under oxygen is challenging

Developing strategies for real time flux measurement and control under oxygen is the key to further improve oxide MBE process reliability